0270-6474/83/0304-0673$02.00/0

The Journal of Neuroscience
Vol. 3, No. 4, pp. 673-702
April 1983

THE LAMINAR ORGANIZATION OF THE LATERAL GENICULATE BODY AND THE STRIATE CORTEX IN THE SQUIRREL MONKEY (*SAIMIRI SCIUREUS*)[1]

DAVID FITZPATRICK,[2] KAZUO ITOH,[3] AND IRVING T. DIAMOND[4]

Department of Psychology, Duke University, Durham, North Carolina 27706

Received June 4, 1982; Revised October 20, 1982; Accepted October 21, 1982

Abstract

The organization of the projection from the lateral geniculate body to the striate cortex in the squirrel monkey has been re-examined using the anterograde and retrograde transport of horseradish peroxidase (HRP) and wheat germ agglutinin conjugated to HRP. The results confirm earlier findings that the projections of the magnocellular and parvocellular layers of the lateral geniculate body terminate in separate sublaminae of layer IV of striate cortex; a more superficial projection of the parvocellular layers to a narrow strip at the base of layer III (IVA in Brodmann's terminology) has also been confirmed. In addition to these well characterized pathways, our results show that the projections of the lateral geniculate body terminate in more superficial levels of layer III and sparsely in layer I of striate cortex. The projections to the upper portion of layer III terminate in distinct patches which coincide precisely with patches of cytochrome oxidase activity previously identified in this zone. The projections to the patches originate primarily from small, pale-staining cells of the "intercalated layers" which surround the magnocellular layers of the lateral geniculate body. A comparison of the organization of the geniculo-cortical projections in the squirrel monkey with that of the cat, *Galago*, and *Tupaia* suggests that, despite marked species differences in the laminar organization of the lateral geniculate body and striate cortex, there are striking similarities in the pathway which terminates in the most superficial layers of striate cortex.

The striate cortex seems to be organized according to a similar plan in distantly related species, the tree shrew (*Tupaia*), the prosimian *Galago*, and the cat. In each of these species layer IV is divided into two tiers, each of which receives fibers from a distinct class of lateral geniculate cells; those lateral geniculate cells, in turn, may or may not be segregated into different layers (Harting et al., 1973; Glendenning et al., 1976; Ferster and LeVay, 1978). The cortex above layer IV is also the target of lateral geniculate axons. The significant point for the present purpose is that the cells of origin for those fibers projecting to layers I to III also have several features in common in the three distantly related species. The source of this projection is from those geniculate layers with the smallest cells: layer 3 in tree shrew, layers 4 and 5 in *Galago* (Carey et al., 1979), and the parvocellular C layers in the cat (Levay and Gilbert, 1976; Levanthal, 1979). These layers receive fine caliber retinal fibers which originate, at least in cat and *Galago*, from a certain type of ganglion cell, the so-called "W" cell class as defined by electrophysiology (Wilson and Stone, 1975; Wilson et al., 1976; Norton and Casagrande, 1982). These layers are also similar in that they receive projections from the superficial layers of the superior colliculus (Niimi et al., 1970; Graham, 1977; Fitzpatrick et al., 1980).

The remarkable similarity in the organization of the striate cortex in these distantly related species suggests that a similar organizational plan should apply to the monkey. Considerable evidence supports the idea that layer IV of the monkey striate cortex is subdivided into two tiers which receive projections from two distinct classes of lateral geniculate neurons (Hubel and Wiesel, 1972; Lund, 1973; Hendrickson et al., 1978). The idea that the superficial layers of striate cortex (above IVA in Brodmann's term) may be the target of a third class of geniculate axons has not been established in the monkey.

[1] This work was supported by National Institute of Mental Health Research Grant 04948 and National Science Foundation Research Grant BNS-7915780 to I. T. D.

[2] Present address: Departmant of Ophthalmology, Medical University of South Carolina, Charleston, SC 29403.

[3] Present address: Department of Anatomy, Kyoto University, Kyoto, Japan.

[4] To whom correspondence should be addressed.

At the same time there have been a number of recent observations that injections of tritiated amino acids into the eye or directly into the geniculate produce a patchy distribution of silver grains in layer III of striate cortex (Weber et al., 1977; Hendrickson et al., 1978; Hubel and Wiesel, 1978).

In the present study, we have re-examined the laminar organization of the projection from the lateral geniculate body to striate cortex in the squirrel monkey by using the retrograde transport of horseradish peroxidase (HRP) and the anterograde transport of wheat germ agglutinin conjugated to HRP (WGA-HRP). The results to be presented confirm that there is a direct projection from the lateral geniculate body to the most superficial layers of the striate cortex which terminates in a discontinuous, "patchy" fashion. This projection arises largely from a distinct class of geniculate neurons which share a number of features in common with the neurons that project to the superficial layers of striate cortex in the cat, *Galago*, and *Tupaia*.

Materials and Methods

Injections of tracers. Injections of wheat germ agglutinin conjugated to horseradish peroxidase (from Sigma) were made bilaterally into the lateral geniculate bodies of eight squirrel monkeys (*Saimiri sciureus*). A 5% solution of WGA-HRP was made by dissolving the WGA-HRP in either 0.1 M Tris buffer containing 2% lysophosphatidylcholine (Sigma type 1) to increase the uptake of tracer or 0.9% saline containing 0.05 to 0.1% poly-L-α-ornithine (Sigma) to limit the size of the injection. The injections were made by iontophoresis (0.5 to 2 μA, 2 pulses/sec, 200 to 300 msec/pulse, 30 to 45 min duration) through glass micropipettes which were pulled and broken to an inner diameter of 5 to 15 μm. Positioning of the injection site within the geniculate was aided by recording (through the injection pipette) the responses of neurons to light flashes in the ipsilateral or contralateral eye.

Restricted iontophoretic injections of HRP were made bilaterally into the striate cortex of four squirrel mon-

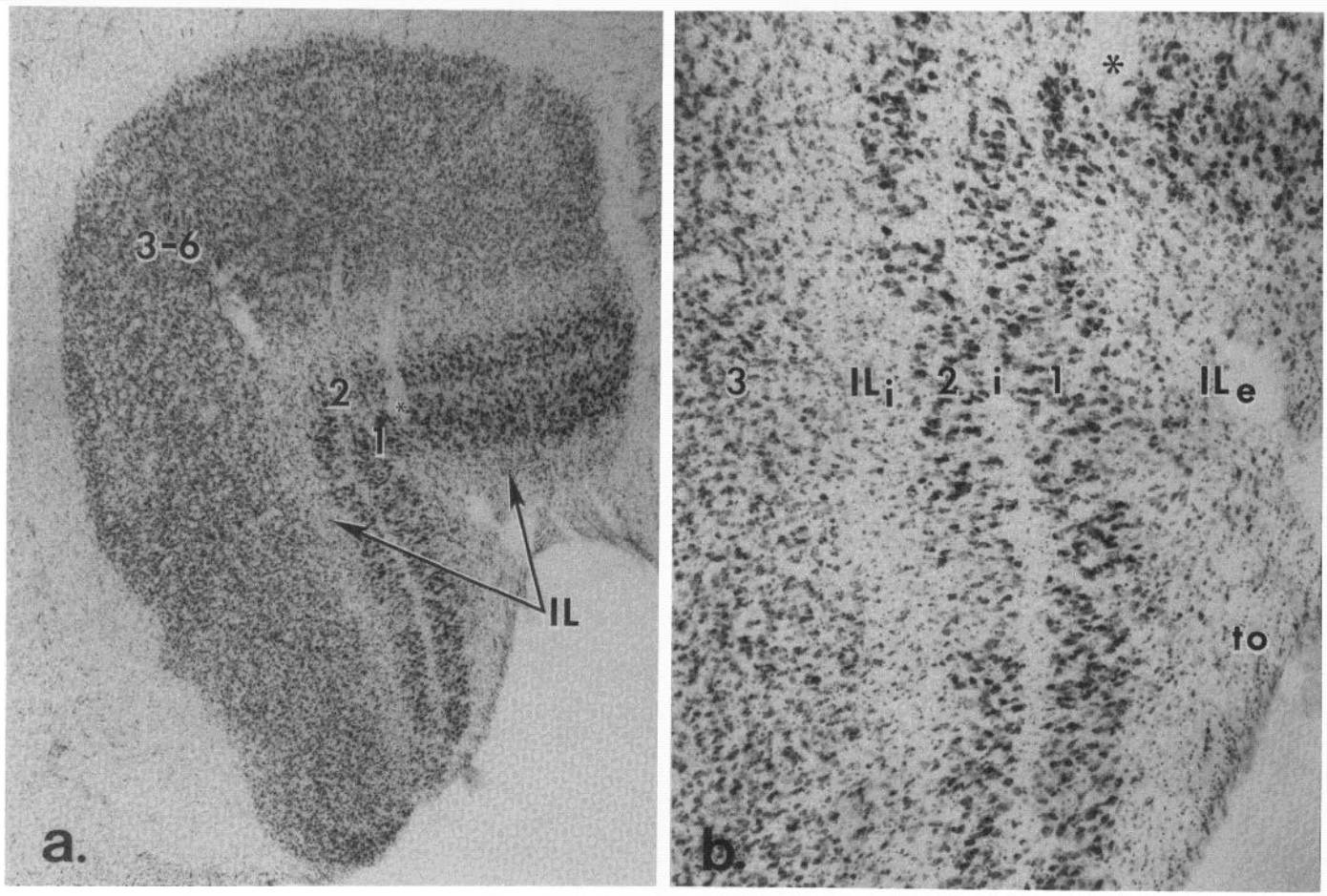

Figure 1. Lateral geniculate body in *Saimiri*. *a*, Low power photomicrograph of a Nissl-stained section through the lateral geniculate body in *Saimiri* showing the prominent magnocellular layers (layers *1* and *2*), the parvocellular mass (consisting of concealed layers *3–6*), and two lightly staining intercalated layers on either side of the magnocellular layers (*IL*) (× 35). *b*, Higher power photomicrograph from the same section shown in *a*. The internal (IL_i) and external (IL_e) intercalated layers consist of small, pale-staining cells. These zones are different from the interlaminar zone (*i*) which contains few neurons (× 80).

keys. A 10% solution of Miles HRP in 0.9% saline containing 0.1% poly-L-α-ornithine was used. Micropipette tip size and stimulation parameters were the same as for the WGA-HRP injections. Generally, several HRP injections were placed in an area of 1 to 2 mm in order to label a sufficient number of cells in the lateral geniculate body. Injections in the most superficial layers (I to IIIB) were made by aligning the filled micropipette tangential to the surface of the cortex and just piercing the pia. Injections into deeper layers were made with vertical penetrations.

Three squirrel monkeys received injections of HRP into the posterior chamber of the eye. Injection volumes ranged from 50 to 100 μl of a 20% solution of HRP dissolved in 0.9% saline containing 2% lysophosphatidylcholine.

Tissue processing. After 48 hr survival, animals were perfused with a solution containing 8% formalin, 2% sucrose in 0.1 M phosphate buffer, pH 7.4. Fixation was followed by a 10% sucrose buffer rinse, after which the brain was removed, frozen, and sectioned at 50 μ. Tissue was reacted for HRP by the de Olmos method (1977) using benzidine dihydrochloride as the chromagen.

Cell measurements. In order to measure the area of the cells in the lateral geniculate body, drawings of individual cells were made with the aid of a camera lucida and a × 100 oil objective. To insure that fragments of cells were not measured, only somas with well defined nucleoli were drawn. Cell bodies were drawn in the focal plane of the nucleolus. From these drawings, the areas of the cells were measured using an Apple graphics tablet and computer. Measurements were made on both frozen (tissue which had been processed for HRP) and celloidin material. Because the results were identical, only the results from the celloidin material are presented here.

Results

Laminar organization of the lateral geniculate body in Saimiri

The photomicrograph in Figure 1 makes it clear that, as a first approximation, the lateral geniculate body of *Saimiri* consists of two main components, the magnocellular and parvocellular layers separated by an interlaminar zone. But the interlaminar zone also contains cells—small and pale staining—and another thin band of small cells lies below layer 1. Even the choice of names, "magnocellular" and "parvocellular," reflects the fact that these truly small cell layers have been overshadowed, if not overlooked. There are some notable exceptions: Le Gros Clark was the first to call attention to the thin bands of small, pale-staining cells on either side of the magnocellular layers in both *Aotus* and *Saimiri.* A drawing from his 1941 paper is presented in Figure 2 because it clearly reveals his conception of three distinct classes of geniculate layers.

Similar zones adjacent to the magnocellular layers of *Macaca* have been described by Guillery and Colonnier (1970). These authors emphasized the fact that the small

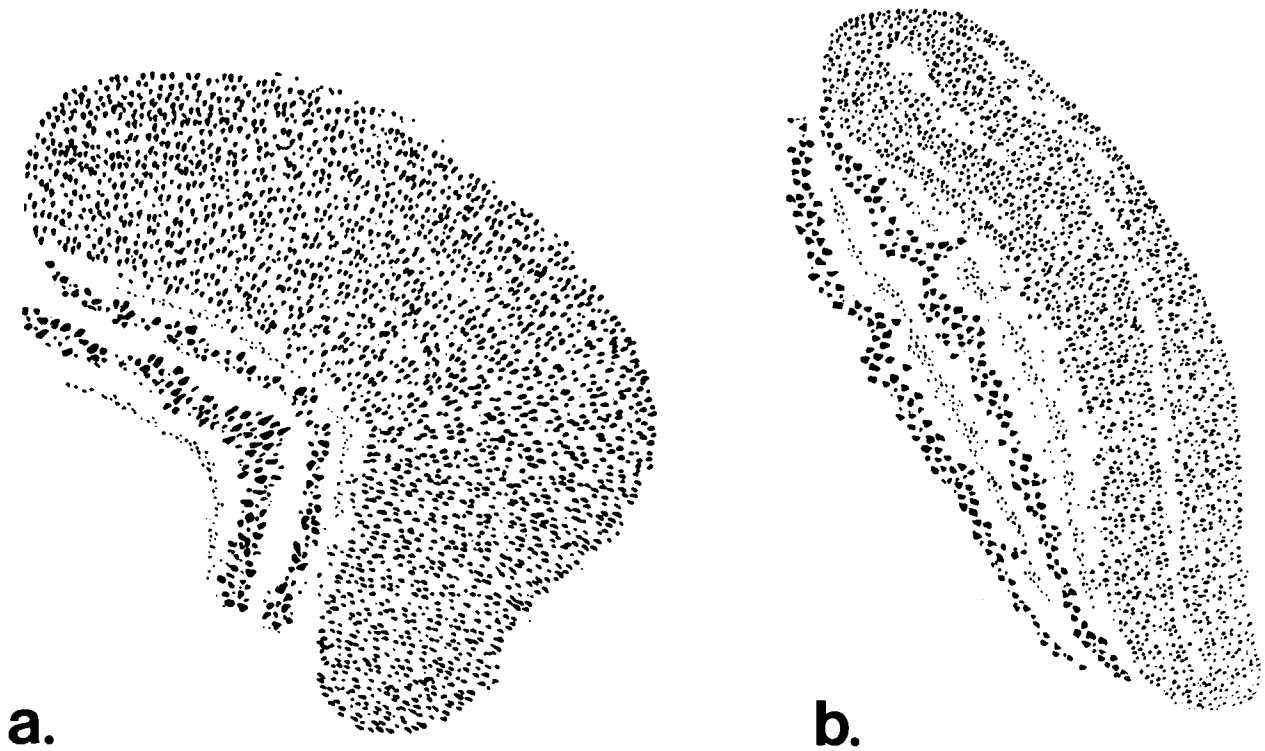

Figure 2. Laminar organization of the lateral geniculate body in *Saimiri* and *Aotus* according to Le Gros Clark. Drawings of Nissl-stained sections through the lateral geniculate body in *Saimiri* (*a*) and *Aotus* (*b*) from the 1941 paper by Le Gros Clark (used with permission from Cambridge University Press). These drawings show his conception of three distinct classes of layers.

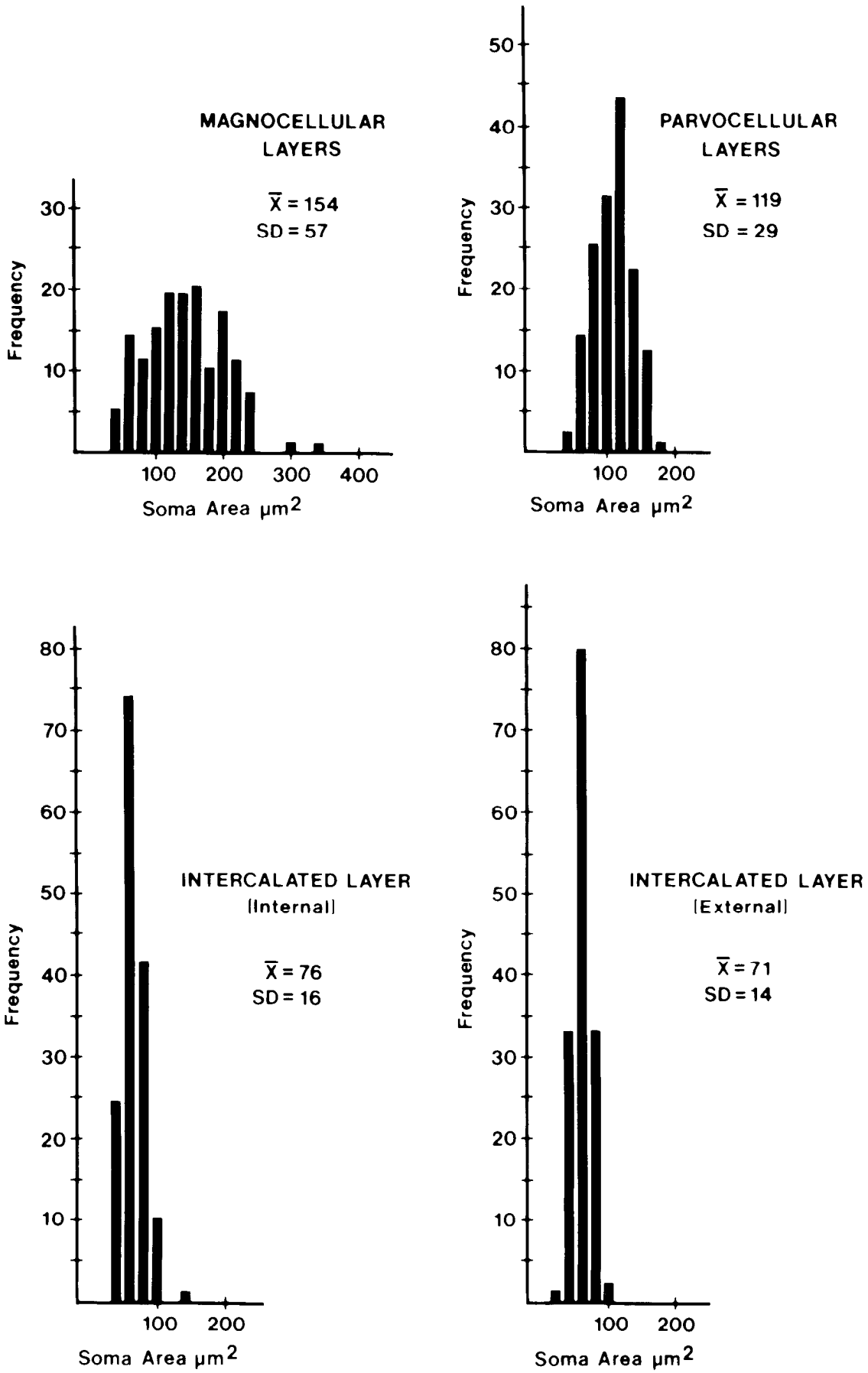

Figure 3. Distribution of cell sizes in the lateral genicualte nucleus of *Saimiri.* Measurements were made on 150 cells from each of the indicated regions.

cell zones show many of the characteristics of the magnocellular and parvocellular layers, including the presence of relatively cell-free strips on either side of the band of cells. Guillery and Colonnier referred to these bands of cells as "intercalated" layers. We have adopted their terminology for both of the small cell zones in *Saimiri* because it confers upon them the status of a layer and indicates something about their position, that is to say, they are inserted between the principal layers or between layer 1 and the optic tract.

Judgments about cell size without measurements can sometimes be misleading, so measurements of cross-sectional area were made for the cells in the magnocellular, parvocellular, and intercalated layers. The results, shown in Figure 3, leave little doubt that there are three distinct and significantly different distributions of cell size. The two distributions taken from the two intercalated layers are almost identical.

There have been several reports of retinal projections to the interlaminar zones surrounding the magnocellular layers of the monkey lateral geniculate body (Hubel et al., 1977; Kaas et al., 1978; Spatz, 1978), and we thought it useful to examine this projection in the squirrel monkey by using the anterograde transport of HRP. The results of one experiment are illustrated in Figures 4 and 5. In the intercalated layer between layers 2 and 3 there is a clear zone of labeled terminals from the contralateral eye (Fig. 4*a*), as well as a less dense zone of ipsilateral input (Fig. 5*a*). A close examination suggests that within this layer the projections from the two eyes are segregated, with fiber terminals from the ipsilateral eye lying predominantly adjacent to layer 2 (Fig. 5*b*) and fiber terminals from the contralateral eye lying predominantly next to layer 3 (Fig. 4*c*). The intercalated layer ventral to layer 1 receives fibers almost entirely from the contralateral retina, and this contralateral input is distributed in a distinctly patchy fashion (Fig. 4*b*). An ipsilateral projection to this zone, if present, is very small and limited to several sections.

The anterograde transport of HRP from the eye also gave us the opportunity to compare the caliber of the labeled processes among different layers of the lateral

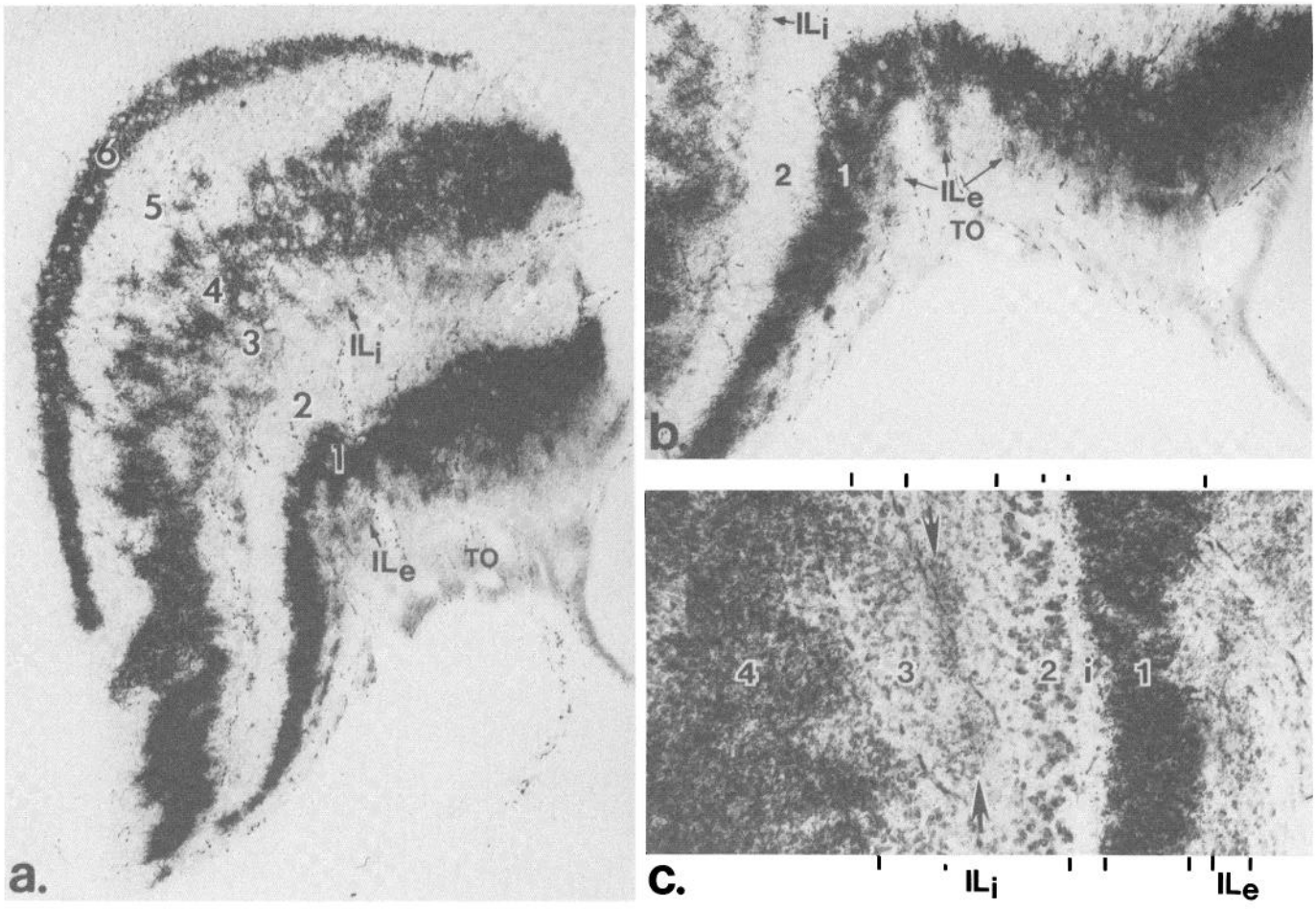

Figure 4. Retinal projections to the lateral geniculate body in *Saimiri*: contralateral projections. *a*, Distribution of labeled terminals in the lateral geniculate body following an injection of HRP into the contralateral eye. In addition to dense projections to layers *1*, *4*, and *6*, there is a less dense projection to the internal (IL_i) and external (IL_e) intercalated layers (× 35). *b*, Higher power photomicrograph from an adjacent section showing discrete "puffs" of terminals in IL_e. A thin strip of terminals in IL_i is also present (× 65). *c*, Photomicrograph from a counterstained section showing the relationship between the retinal terminals in IL_i (*arrows*) and layer *2* and layer *3*. The projections from the contralateral eye terminate near layer *3*, leaving a blank zone next to layer *2*. Note the presence of lightly labeled terminals in IL_e and the lack of terminals in the interlaminar zone (*i*) (× 95).

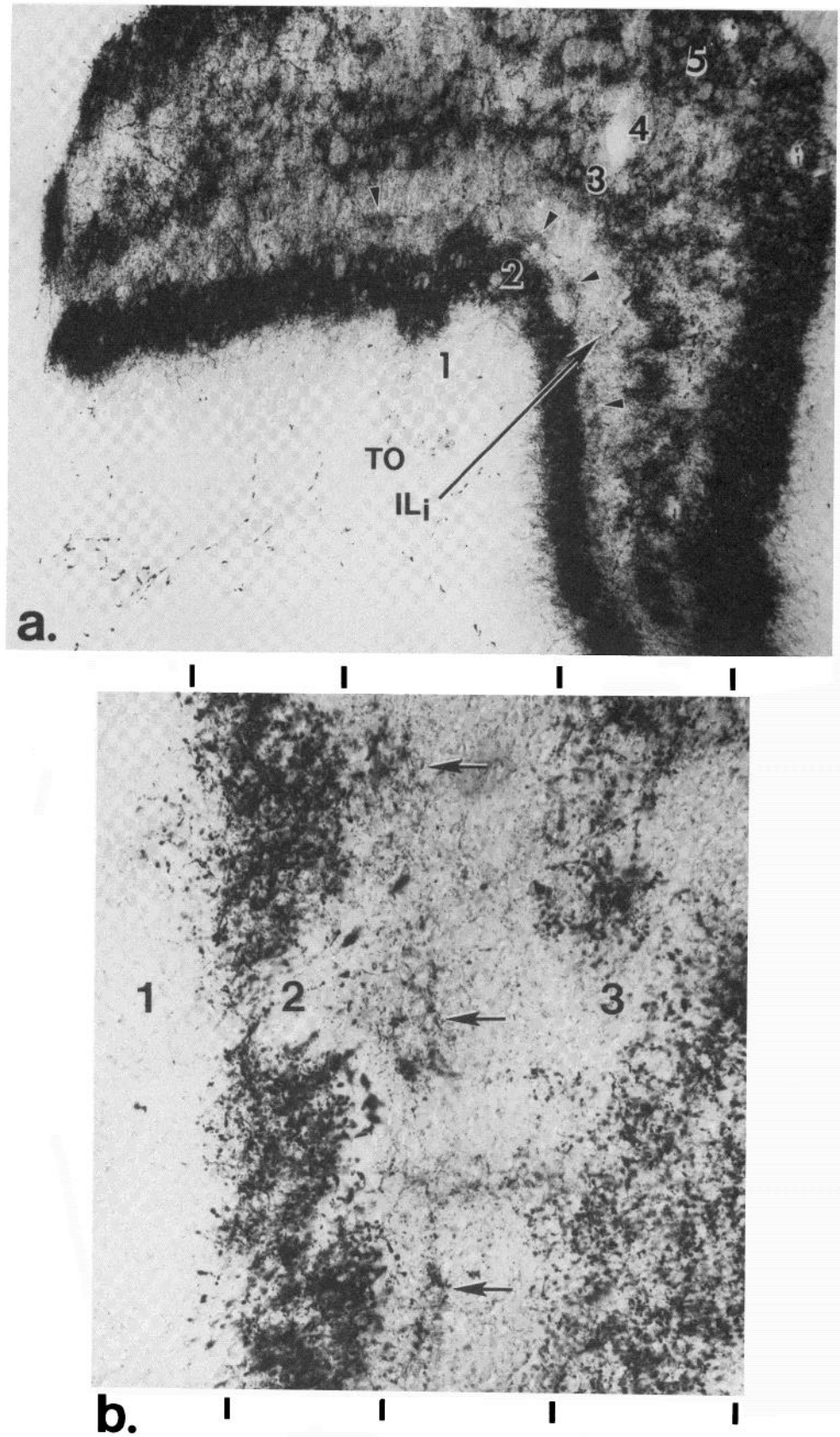

Figure 5. Retinal projections to the lateral geniculate body in *Saimiri*: ipsilateral projections. *a*, Distribution of labeled terminals in the lateral geniculate body following an injection of HRP into the ipsilateral eye. In addition to dense terminals in layers *2*, *3*, and *5*, there is a less dense projection to IL_i (*arrowheads*) (× 50). *b*, Higher power photomicrograph showing the relationship between retinal terminal clusters in IL_i (*arrows*) and layers *2* and *3*. The terminals are located next to layer *2*, leaving a blank zone next to layer *3*. Compare with Figure 4*c* (× 180).

geniculate nucleus (Fig. 6). Within the magnocellular layer large bulbous terminals are present, whereas the terminals within the parvocellular layers are slightly smaller. A difference in the size of retinal terminals in the magnocellular and parvocellular layers has also been observed by Guillery and Colonnier (1970) in *Macaca*. In contrast, very fine caliber processes predominate within the intercalated layers. Of course, these observations do not rule out the possibility that fine caliber processes are also present within the magnocellular and parvocellular layers or that the fibers projecting to the intercalated layers are collaterals of axons that terminate in the principal layers. But the difference in the size of terminals, taken with other evidence of cell size and staining intensity, does suggest that the intercalated layers may be the recipient of a separate class of retinal input.

Up to this point, the similarity between the intercalated zones on either side of the magnocellular layers has been emphasized. However, the cells below layer 1 require a further and more detailed analysis because they actually consist of two separate and distinct regions, and it is of crucial importance to the argument that these not be lumped together, as is a common practice, into a single "S" layer or "O" layer.

In addition to the pale-staining band of small cells which has been described, at certain levels of the nucleus (and this level seems to vary) a cluster of very large, dark-staining cells appears between layer 1 and the optic tract. This large cell cluster is further distinguished from the small cells of the intercalated layer on the basis of retinal input: the large cell cluster receives *large* caliber terminals from the *ipsilateral* eye, whereas the intercalated layer receives *fine* caliber terminals from the *contralateral* eye. The results to be presented next will show that this large cell cluster is actually a displaced portion of layer 2, a point recognized by Casagrande and Joseph (1980) in their studies of the large cell "S" layer in *Galago*.

Figure 7 shows the transport of HRP from the eye to the ipsilateral and contralateral geniculate bodies. Layers containing HRP-labeled terminals are shown in *black*; unlabeled zones are shown as *stipple*. Section 50 on the side ipsilateral to the eye injection shows two distinct targets of the ipsilateral eye separated by the unlabeled geniculate layer. Undoubtedly, this separate zone of ipsilateral input lying ventral to layer 1 would have been called the "S" layer. However, if the "S" layer and layer 2 are traced caudally in successive sections, it is clear that these two separate regions are actually continuous. It seems that layer 1 becomes divided and that portions of layer 2 pass through the point of division. A very similar picture is apparent on the contralateral side. Photomicrographs of section 48 on the ipsilateral and contralateral sides are presented in Figure 8.

A slightly different pattern of association between the ventral large cell cluster and layer 2 is shown in Figure 9. In this case, the cluster of large cells and terminals occurs in the middle of the nucleus (section 78). At more caudal levels, the cluster breaks up into smaller pieces, and these patches appear to pass through layer 1 and become continuous with an evagination of layer 2.

Several pieces of evidence suggest that the S layer, as this term was *originally* used, designated just the displaced portion of layer 2. First, the S layer was thought to receive just ipsilateral projections (Campos-Ortega and Hayhow, 1970; Giolli and Tigges, 1970). The present results show ipsilateral projections to the cluster of large cells that lies below layer 1, but contralateral projections to the small cells of the intercalated layer. Second, the large cells overshadow the small cells. Indeed, there are accounts of transneuronal degeneration of the S layer

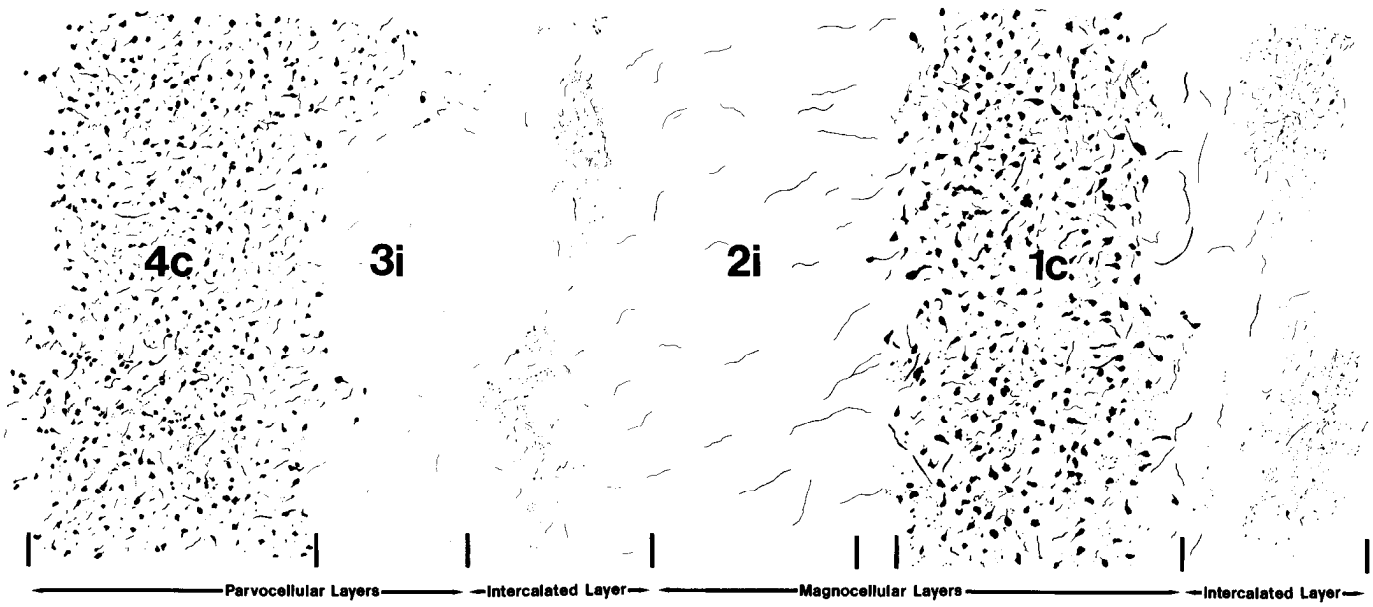

Figure 6. Caliber of retinal terminals in the lateral geniculate body. Camera lucida drawing of HRP-labeled terminals in the lateral geniculate nucleus following an injection of HRP into the contralateral eye. Layers 5 and 6 have been omitted. The retinal terminals in the magnocellular layers are the largest, the terminals in the parvocellular layers are intermediate, and the terminals in the intercalated layers are distinctly fine (× 225).

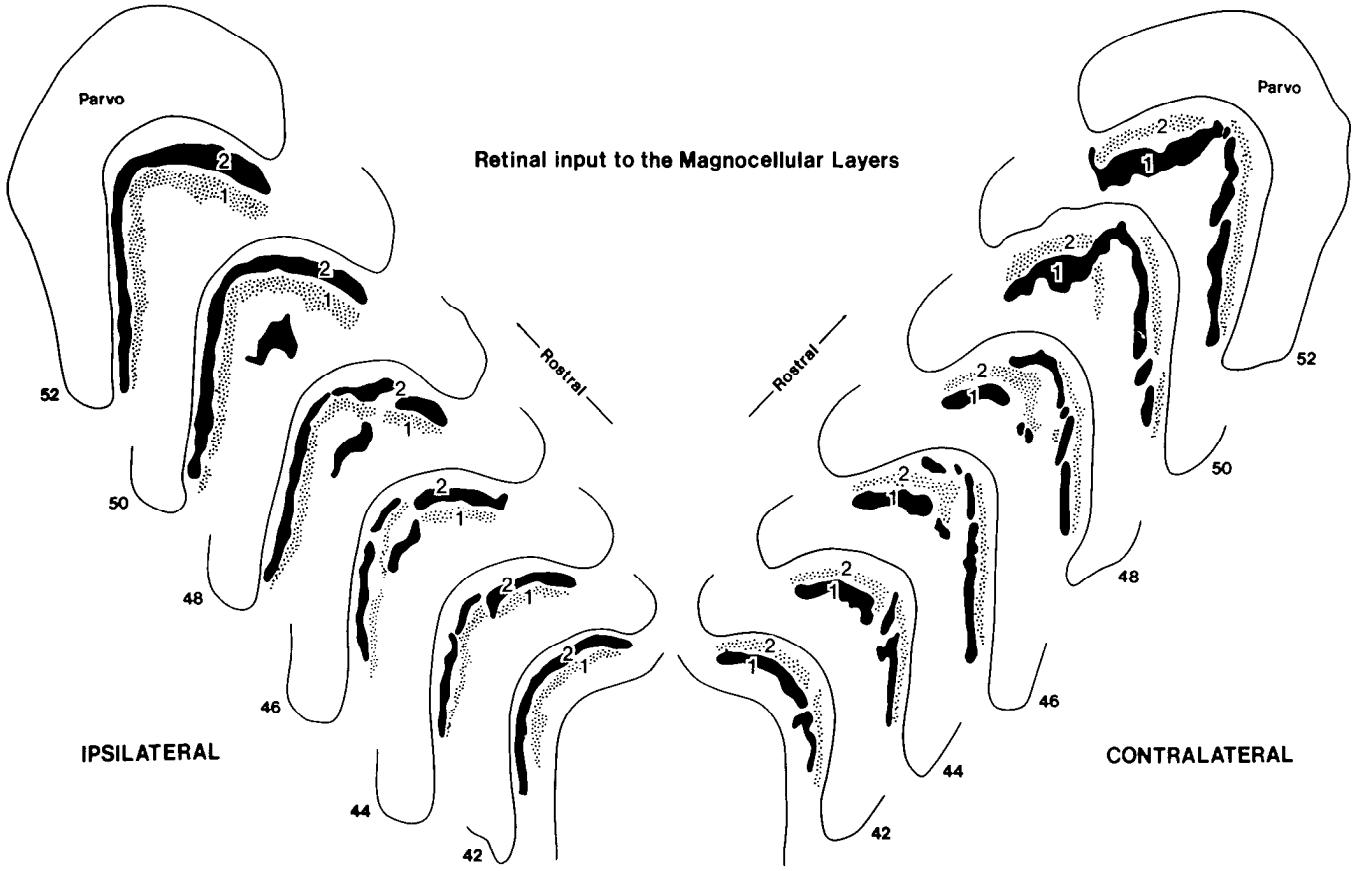

Figure 7. Retinal input to the magnocellular layers. Drawings of frontal sections through the lateral geniculate body in *Saimiri* showing the retinal input to the magnocellular layers. This figure shows the way in which a portion of layer 2 extends through and below layer 1. *Black* indicates layers which contain labeled terminals; *stipple* represents unlabeled layers. The most caudal section is *#42*. The most rostral section is *#52*. Photomicrographs of section *48* are shown in Figure 8.

following removal of the ipsilateral eye, and it is hard to imagine that changes of this sort would have been detected in the small, pale-staining zones referred to here as intercalated layers (Chacko, 1955; Giolli and Tigges, 1970). Third, degeneration methods may not have been sensitive enough to detect the fine caliber terminals that characterize the intercalated layer, but they would have shown the large caliber projections to the displaced portion of layer 2.

Displacements of the magnocellular layers have been noted in the lateral geniculate nucleus of man (Hickey and Guillery, 1979) and chimpanzee (Tigges et al., 1977a), and a complex branching pattern of the parvocellular layers has been shown (Kaas et al., 1978). The displacement of the magnocellular layers in *Saimiri* is often associated with the presence of large blood vessels entering the hilus of the lateral geniculate, and that could be some clue to the cause (see Fig. 8). Whatever factors are responsible for the displacement, the intercalated layer below layer 1 is clearly a separate entity consisting of small cells that are targets of fine caliber retinal input chiefly from the contralateral eye.

The striate cortex in Saimiri

Before presenting the results of experiments designed to trace the projections of geniculate layers to cortex, it is necessary to describe the laminar organization of the striate cortex. Because the names we give to some of the layers of the striate cortex differ from those most commonly used, our choice of terms must be defended. Discussions about nomenclature are often apologetic, apparently because what a structure is called seems less significant than what functions it serves or what connections it has. But if terminology reflects an effort to reveal homology and connections, an appropriate name for a structure is one of the goals of the inquiry.

The terminology presented here is based on relating the study of cytoarchitectural features to the laminar organization of the connections of striate cortex in *Saimiri*. Using *both* cytoarchitecture and connections to define the laminar organization of striate cortex poses a problem, because, in order to define the subdivisions, reference must be made to the results of connectional experiments, but to present the results of connectional experiments using prevailing terminology would only confuse the issues. In order to avoid this problem, photomicrographs of several Nissl-stained sections through the striate cortex are presented in Figure 10, and the present terminology is described by anticipating the connectional evidence that will be presented in the next section.

As in most primates the most conspicuous feature in

the striate cortex of *Saimiri* is the very dark band of small cells that is characteristic of layer IV in most cortical areas. Immediately superficial to the densely populated band of dark-staining cells is a less populated light zone with pale-staining cells. We take issue with the previous terminology chiefly in the name applied to this light-staining band. In the terminology used by Hassler and Wagner (1965) and Tigges et al. (1977b), this light-staining zone is considered a part of IIIC, whereas those who follow Brodmann's school (1905), such as Colonnier and Sas (1978), refer to it as a subdivision of IVB. Both schools agree that the light-staining band corresponds to the stripe of Gennari, with the implication that it is *not* a major target of projections from the lateral geniculate body. Our results show quite the contrary—that this light-staining zone is the target of axons from the magnocellular layers. Furthermore, the cells that comprise this layer appear small and spherical in Nissl-stained material and are only slightly larger than cells in the subadjacent dark band. For these reasons we call the pale-staining zone IV_α. This zone appears to be equivalent to ICV_α in the macaque as defined by Lund (1973).

The dark-staining band of cells immediately below IV_α is simply called "layer IV" in the Hassler terminology (Hassler and Wagner, 1965) and "layer IVC" in the Brodmann terminology (1905). The concentration of small cells in this band is not uniform but is greater at the base. Without the benefit of knowing the targets of the magnocellular and parvocellular layers, it might be tempting to relate this slight difference in density to the difference in the projections from the magnocellular and parvocellular layers. However, as the results will show, the entire extent of the dark band is the target of the parvocellular layers and will be referred to here as IV_β (which corresponds to IVC_β in the Lund (1973) terminology).

We draw the upper border of IV_α just below a conspicuous strip of large, dark-staining cells, many of which appear to be pyramidal cells. The presence of large pyramidal cells marks the dorsal border of layer IV not only in the striate cortex of other species but in other cortical areas, and, to be consistent with this scheme, the strip of cells and the light band immediately above it are called IIIC. Our results show that layer IIIC is not a direct target of the lateral geniculate body. Layer IIIC is further distinguished by its projection to the middle temporal area (MT) (Spatz, 1977; Tigges et al., 1981).

The layer immediately above IIIC has a distinctly granular appearance which is best seen in Figure 10*c*. To be sure, granular cells are not the only cell type found in this layer, but the small size of the cells and the increased density of the population clearly define a separate layer.

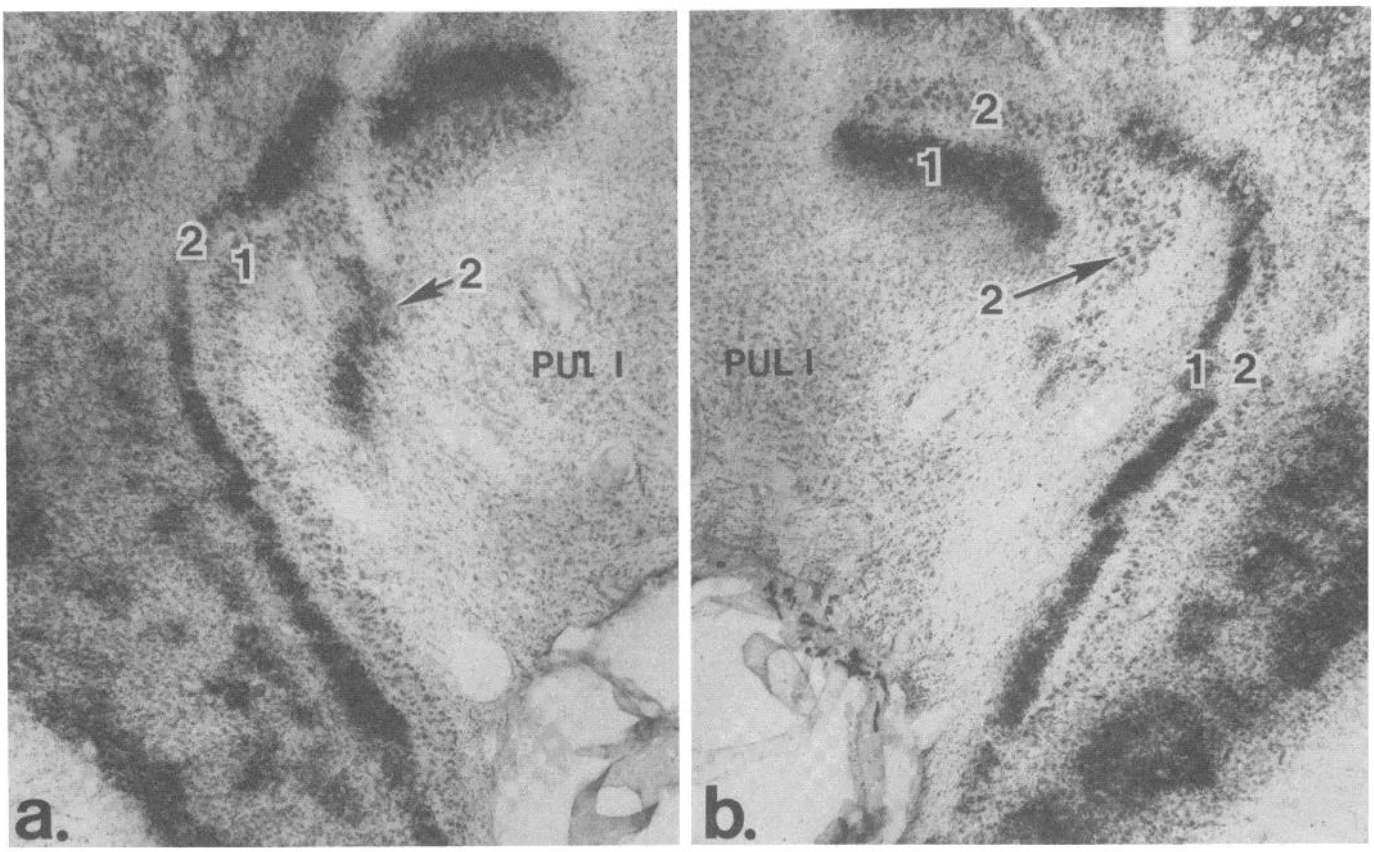

Figure 8. Retinal input to displaced portions of the magnocellular layers. *a*, This photomicrograph is from section 48 (illustrated in Fig. 7) and shows a large cluster of terminals (*arrow*) overlying magnocellular neurons which lie ventral to layer *1*. This section shows the retinal input from the ipsilateral eye (× 70). *b*, Same section as in *a*, but this shows the retinal input to the contralateral lateral geniculate body. Unlabeled layer 2 (*arrow*) is seen lying between two separate segments of layer *1* (× 70).

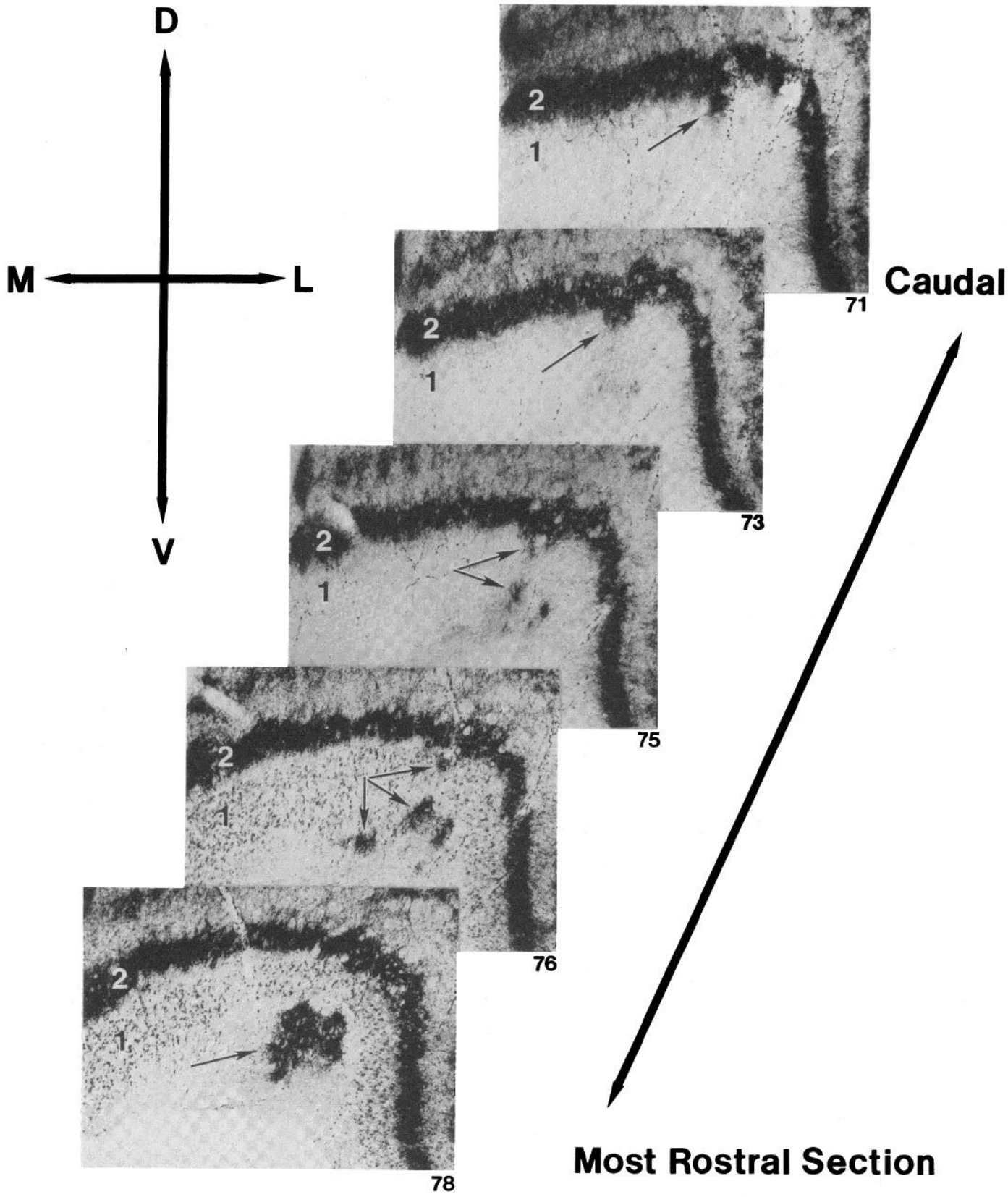

Figure 9. Displacement of magnocellular layer 2: a second pattern. Closely spaced frontal sections through the lateral geniculate of *Saimiri* which received an injection of HRP into the ipsilateral eye. A small evagination seems to emerge from the ventral aspect of layer *2* (sections *71*, *73*) At more rostral levels, this evagination breaks up into several clusters which pass through layer *1* and eventually coalesce into a large cluster (section *78*) ventral to layer *1* (× 35).

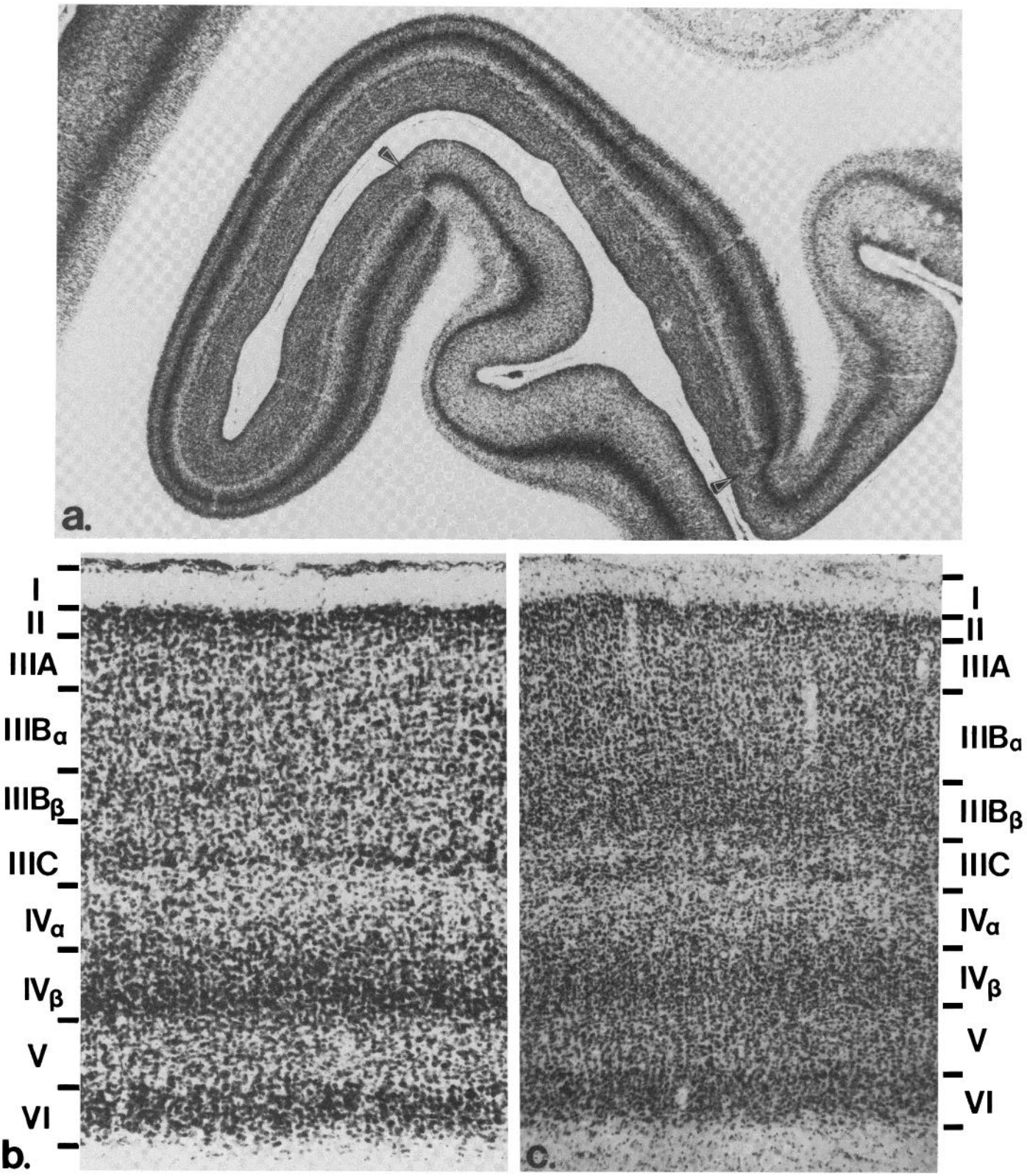

Figure 10. Cytoarchitecture of striate cortex in *Saimiri*. *a*, Low power photomicrograph of a section through the striate cortex surrounding the calcarine fissure. The *arrowheads* point to the borders of area 17 with area 18. This is from a celloidin section stained with cresyl violet (× 15). *b*, Higher power photomicrograph from the same section illustrated in *a*. This photomicrograph illustrates a difference in the density of the cells within IV_β and the large size of the cells in *IIIC* (× 70). *c*, Frozen section through striate cortex stained with neutral red. This section shows the difference in cell packing density and size which characterize the subdivisions of layer III. Why layer $IIIB_\beta$ looks more granular in frozen sections is obscure. For comparison with the Brodman (1905) terminology as modified by Lund (1973): IV_β = IVC_β; IV_α = IVC_α; *IIIC* = IVB; $IIIB_\beta$ = IV_A (× 70).

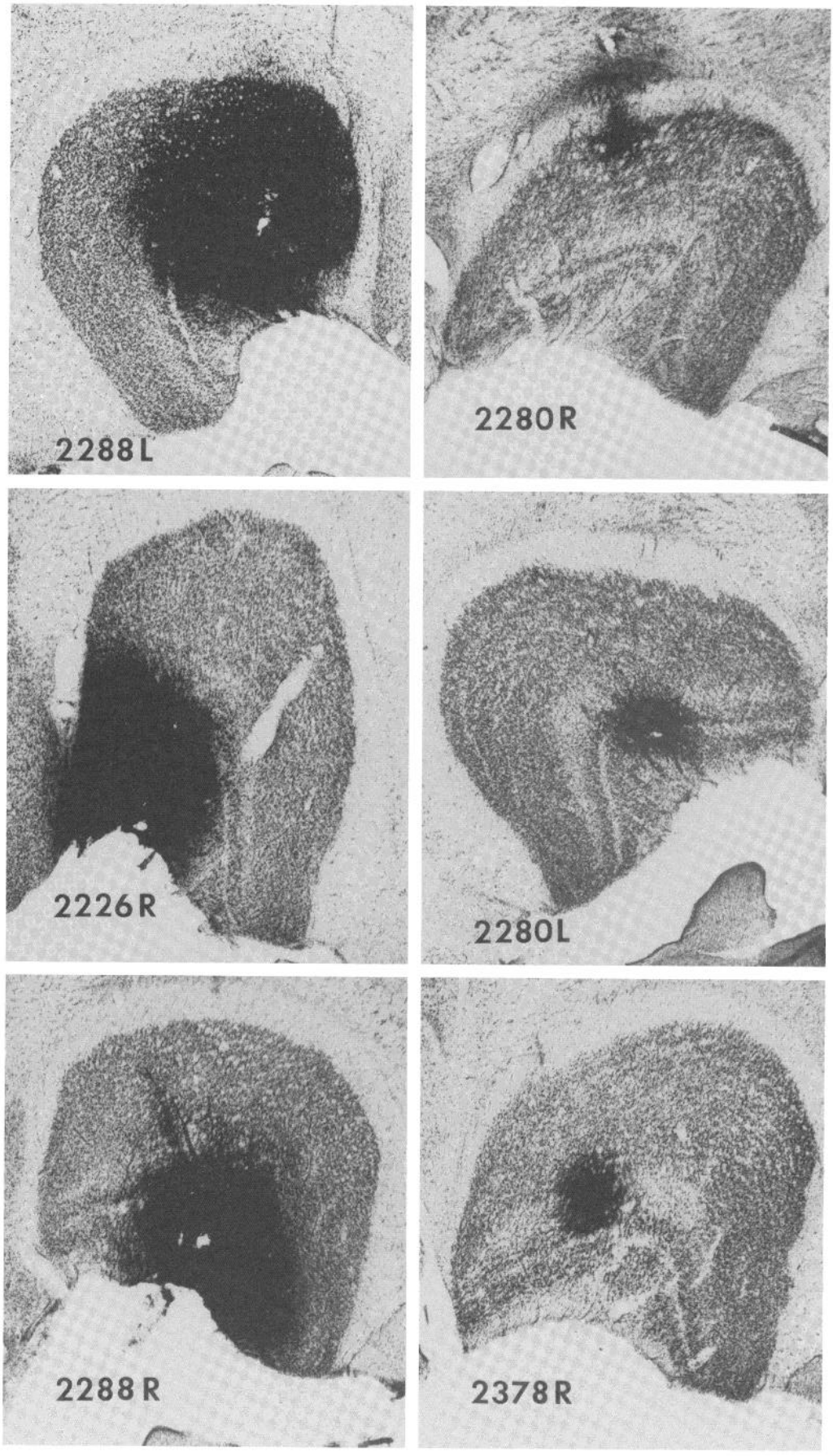
2288L
2280R
2226R
2280L
2288R
2378R

We have no objection to the term "IVA" for the upper granular layer as a way of indicating its similarity to the lower granular layer. We do object to using the name "IVB" for the region between the two granular layers because that would obscure the similarity between the pyramidal cell layer (our IIIC) and the base of layer III in other cortical areas. Even more significant, the term "IVB" obscures the homology of this zone with similar layers in the striate cortex of other species such as *Galago* that have no well defined upper granular tier.

In order to avoid a nomenclature in which layer IIIC lies between two sections of layer IV, we decided to call the upper granular tier a separate part of layer IIIB ($IIIB_\beta$). The results below will show that the base of this zone receives a direct projection from the lateral geniculate body, and this layer is also distinguished by a projection from the stellate cells of layer IV. The upper part of IIIB, $IIIB_\alpha$, is also a target of the lateral geniculate body, and it is important to note that it is the primary source of projections to area 18 (Tigges et al., 1981; D. Fitzpatrick and K. Itoh, experiments in progress). The border between $IIIB_\alpha$ and IIIA is not sharp, but, following injections of HRP into area 18, few labeled cells are found in IIIA. In the Nissl-stained section, layer IIIA appears to consist of a smaller class of pyramidal cells than those in IIIB. Finally, layer IIIA is bounded dorsally by the thin band of darkly staining cells comprising layer II.

Laminar organization of geniculo-striate projections

Total pattern of geniculate terminals in striate cortex. In order to see the entire pattern of geniculate terminals, large injections of WGA-HRP were made into the lateral geniculate nucleus of several animals. The injection site for one of these cases (case *2288L* shown in Fig. 11) involved all layers of the lateral geniculate nucleus but did not spread into the pulvinar nucleus. Labeled terminals from this experiment were distributed throughout a wide sector of the calcarine fissure, and Figure 12*a* shows a low power darkfield photomicrograph of these labeled terminals. The broad labeled band of terminals in the middle of the cortex corresponds to layers IV_α and IV_β. Superficial to this broad band of terminals is a zone—IIIC—that is virtually devoid of terminals. Superficial to layer IIIC is a very thin band of terminals that lies just at the base of $IIIB_\beta$. Projections to the base of $IIIB_\beta$ as well as to layer IV have been described by other investigators (Hubel and Wiesel, 1972; Lund, 1973; Tigges et al., 1977b; Hendrickson et al., 1978). More significant for our special interest in projections superficial to layer $IIIB_\beta$ is the distribution of terminals in discrete patches, the centers of which are separated by roughly 400 μm. The patches of label appear to lie chiefly within the zone that we have defined as $IIIB_\alpha$; however, they are not confined to this zone and in some sections they extend almost to the terminal band in $IIIB_\beta$ and continue into $IIIB_\alpha$ (Fig. 12*c*).

In another experiment, the injection site involved more caudal levels of the geniculate, and this allowed us to examine the distribution of geniculate patches in a more oblique plane. Figure 12*b* shows the mosaic pattern they form across the cortical surface. Each patch is cylindrical in shape, and the distances between adjacent patches are uniform.

In addition to the patchy projection to layer III, a sparse distribution of terminals was noted in the upper portion of layer I. While layer I in Figure 12*a* appears to have a large number of labeled terminals, the lightness of this zone is an edge artifact due to the low power darkfield condensor. The actual density of terminals in layer I is best represented by the higher power photomicrograph in Figure 12*c* that is taken from the same section.

In addition to labeled terminals in the superficial layers, a large number of labeled cells were found in layer VI. The presence of these labeled cells makes it impossible to say whether there are also geniculate terminals in this layer.

The precise relation between the axon terminals of lateral geniculate neurons and the boundaries of layers $IIIB_\beta$, IIIC, and IV is shown in Figure 13. In Figure 13*b* the *arrows* point to two conspiciously large cells which lie at the lower border of layer IIIC. By comparing the position of these cells with the extent of terminals revealed in the darkfield photomicrograph (Fig. 13*a*), it is apparent that geniculate terminals occupy a wide zone which begins at the bottom of the dark granular layer IV and ends just below the base of the large cells that lie in layer IIIC. No geniculate terminals are found within this band of cells or in the cleft which lies dorsal to the strip of cells. A second zone of geniculate terminals does appear just at the base of $IIIB_\beta$. Thus, the extent of geniculate terminals supports the proposed definition of layer IV: it is the zone bounded by the pyramidal cell layer above and layer V below. In the darkfield photomicrograph, a difference in the density and caliber of the terminal field in the upper and lower portions of layer IV can be seen. The next section will show that this difference reflects the difference between the magnocellular projections to IV_α and the parvocellular projections to IV_β.

The contributions of the various layers of the lateral geniculate to the total pattern. The contribution of the various layers of the lateral geniculate body to the total pattern was studied in two ways: first, by restricting WGA-HRP to certain layers of the lateral geniculate body, and second, by restricting HRP to certain layers of the striate cortex.

Case *2226R* illustrates the results of an injection of WGA-HRP aimed at the magnocellular layers. Figure 14 shows that the injection site included the intercalated layer *below* layer 1 but only slightly encroached on the internal intercalated layer between layers 2 and 3 in the most dorsal medial part of the nucleus. The parvocellular layers were largely spared. A band of labeled terminals is found in layer IV_α, patches of labeled terminals are present in layer III, and sparse terminals are present in layer I. A photomicrograph of the injection site and the

Figure 11. Injection sites of WGA-HRP into the lateral geniculate body in *Saimiri*. These photomicrographs show the center of the injection site from each of the cases illustrated in this paper (× 15).

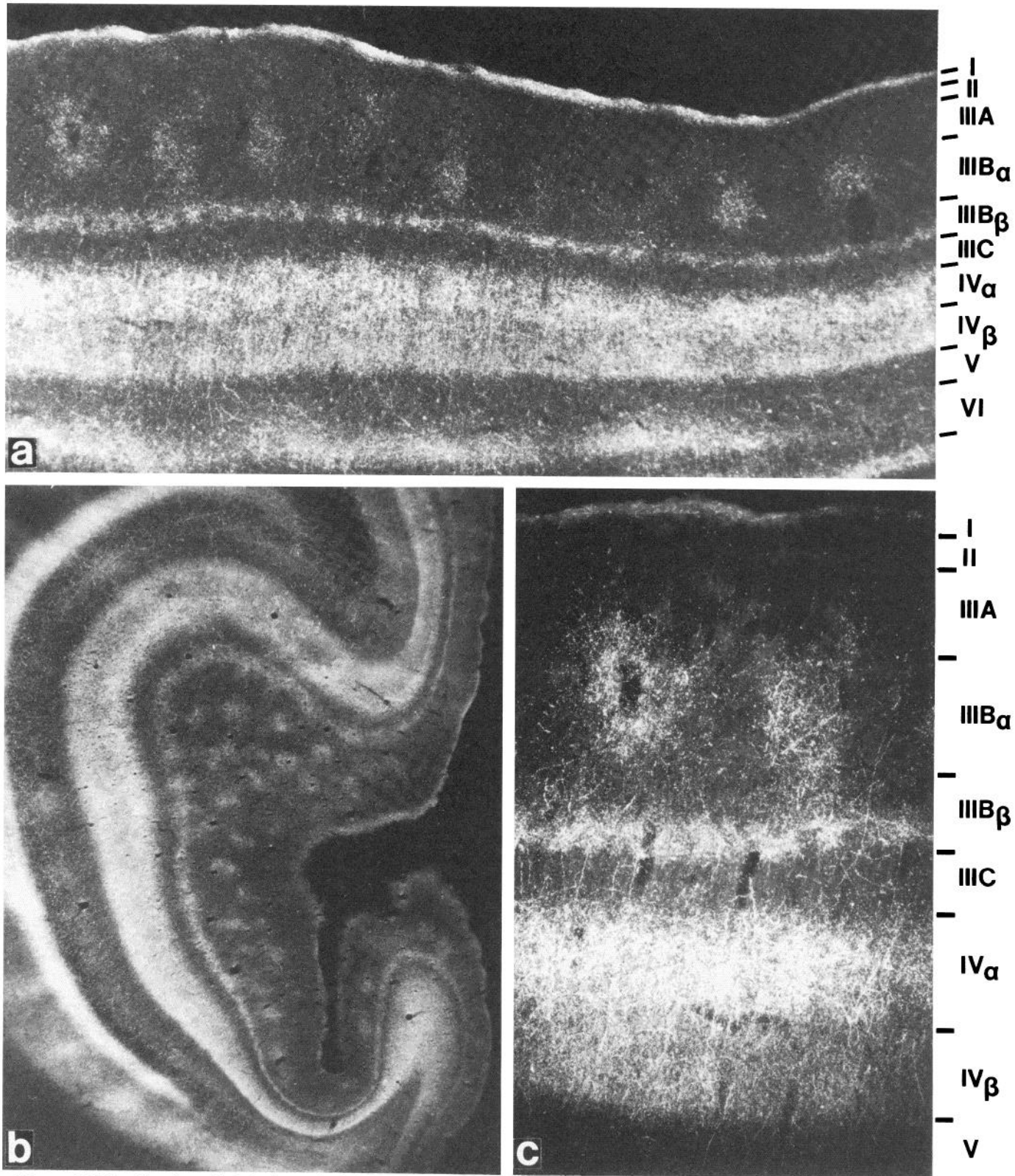

Figure 12. Distribution of labeled terminals in striate cortex following a large injection of WGA-HRP into the lateral geniculate body. *a*, Low power darkfield photomicrograph showing the laminar distribution of terminals from the lateral geniculate body. In addition to projections to both subdivisions of layer IV, and to the base of $IIIB_{\beta}$, there is also a patchy projection to layer III. The lightness of layer *I* in this photomicrograph is largely an edge artifact associated with the low power darkfield condensor. The actual density of terminals in layer *I* is shown in *c*, which is taken from the same section (× 45). *b*, Low power darkfield photomicrograph of a section through the caudal part of the calcarine fissure following a large injection of WGA-HRP into the lateral geniculate body. In this section layer III is cut obliquely, and the mosaic-like distribution of terminal patches within this layer can be seen (× 10). *c*, Higher power photomicrograph from the same section illustrated in *a*. The patch in $IIIB_{\alpha}$ on the right appears to have continuity with the band of terminals in $IIIB_{\beta}$, whereas the patch on the left appears separate. A few terminals are present in the outer half of layer I (× 90).

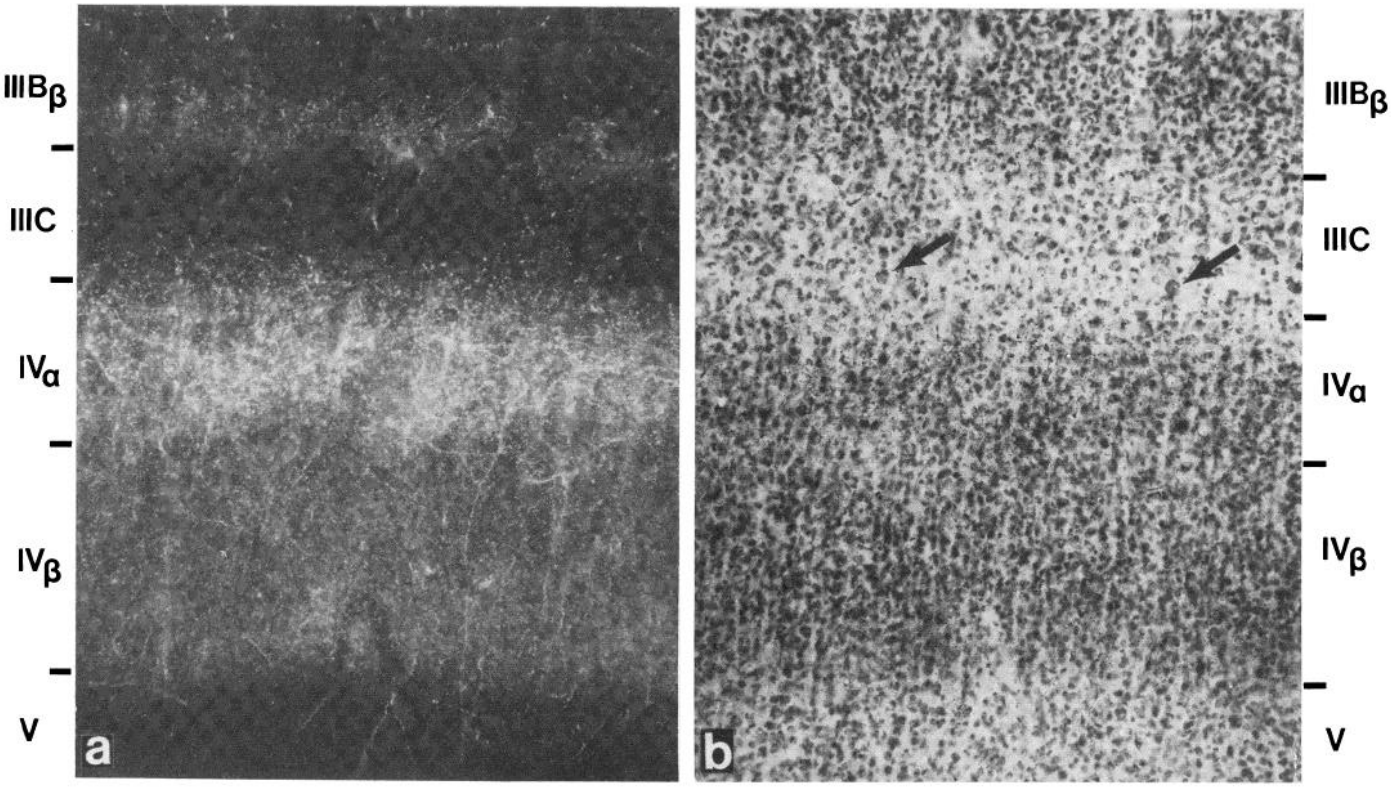

Figure 13. Distribution of geniculate terminals in relation to the cytoarchitecture of the striate cortex. These darkfield (*a*) and lightfield (*b*) photomicrographs show the same portion of a section through the striate cortex following a large injection of WGA-HRP into the lateral geniculate body. The *arrows* point to two large cell bodies which define the lower boundary of *IIIC*. Terminals from the lateral geniculate body end just below the level of these cells. The difference in the caliber of the input to IV_α and IV_β reflects the projection of the magnocellular and parvocellular layers, respectively (× 95).

transport to cortex is shown in Figures 11 and 15, respectively.

The relation between the border of the terminals arising from the magnocellular layers and the border between IV_α and IIIC is indicated more precisely in the photomicrographs of Figure 16. The *arrow* in the lightfield photomicrograph points to a large cell which lies within IIIC. The upper border of the labeled terminals lies just below this cell. No labeled terminals were found in IV_β, whereas IV_α was densely filled with terminals.

The results of an injection of WGA-HRP into the parvocellular layers are illustrated by experiment *2280R* in Figure 17. The injection site involves the most dorsal part of the parvocellular layers but does not involve the magnocellular or intercalated layers. Labeled terminals are found within IV_β and in the band at the base of $IIIB_\beta$. No labeled terminals were found above $IIIB_\beta$.

From these two experiments, the dorsal parvocellular layers can be ruled out as a source of the patches in $IIIB_\alpha$ and the magnocellular layers and the intercalated layer *below layer 1* can be ruled out as the source of the band at the base of $IIIB_\beta$. Furthermore, the results support the idea that the magnocellular layers project to IV_α and the parvocellular layers project to IV_β and to $IIIB_\beta$.

Two additional experiments, *2288R* and *2280L*, provide more information on the source of the projections to $IIIB_\alpha$ and $IIIB_\beta$ (Figs. 18 and 19). In these experiments the internal intercalated layer was included in the injection site, but the parvocellular layers were spared. In both cases no labeled terminals were found in IV_β (as one would expect), yet labeled terminals were found both at the base of $IIIB_\beta$ and in the patches of $IIIB_\alpha$. This finding suggests that the labeled terminals at the base of $IIIB_\beta$ following large injections of the geniculate are not solely the result of the involvement of the parvocellular layers and that the internal intercalated layer may also contribute to the axon terminals at the base of $IIIB_\beta$.

One final anterograde experiment (*2378R*) (see Fig. 20) also supports the idea that the internal intercalated layer sends a projection to $IIIB_\beta$ as well as $IIIB_\alpha$. In this experiment, the injection site is centered in the internal intercalated layer with a slight involvement of layers 2 and 3 on either side. Labeled terminals were found in both subdivisions of layer IV as well as in the base of $IIIB_\beta$ and in the patches of $IIIB_\alpha$. However, two features of this case support the idea that the labeled terminals in the superficial layers are due to the involvement of the internal intercalated layer. First, the labeled terminals in $IIIB_\beta$ and $IIIB_\alpha$ extended over a wider area of the cortex than the terminals in layer IV. Second, except for the center of the region which contained labeled terminals, the projection to the superficial layers was more dense than the projection to layer IV. This is particularly clear in the photomicrograph shown in Figure 21*a*. In the central region, the projection to layer IV was about equal in density to the projection to the more superficial layers (Fig. 21*b*). In the case of large injections of WGA-HRP which include all layers of the geniculate, the projection

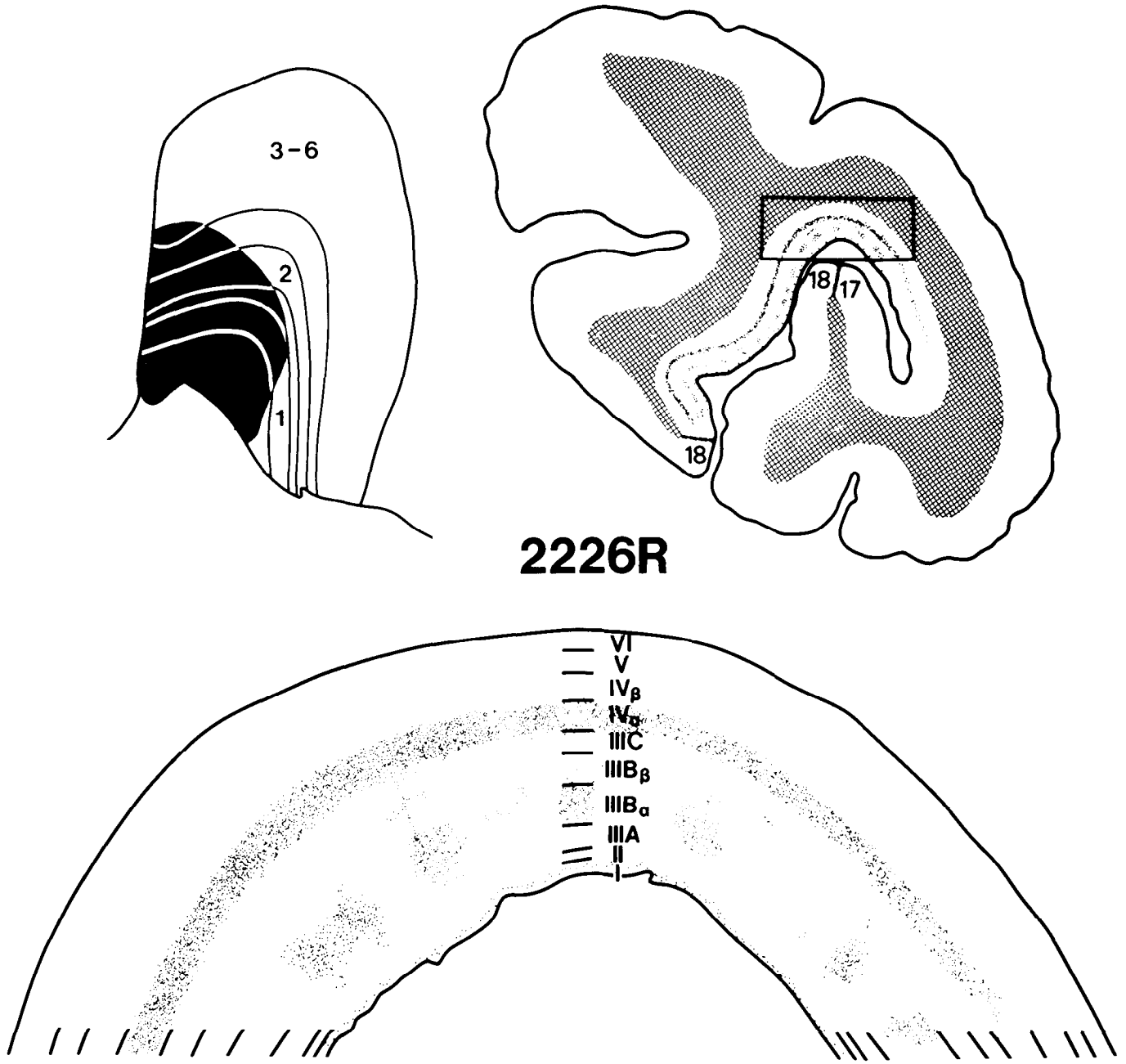

Figure 14. Case *2226R:* Results of an injection of WGA-HRP into the ventral layers of the lateral geniculate body. A photomicrograph of the injection site is shown in Figure 11. A photomicrograph of the labeled terminals in striate cortex is shown in Figure 15.

to layer IV appears more dense than the projection to layer III (see, for example, Fig. 12*a*).

There is one additional feature of this case that is worth noting. In the center of the zone which contained labeled terminals (Fig. 21*b*), the labeled terminals in IV_β were clearly arranged in patches separated by terminal-free zones. This arrangement is reminiscent of ocular dominance patches which are found in other species and may be related to the involvement of ipsilateral parvocellular layer 3 in the injection site without the involvement of layer 4. Although transneuronal transport studies have failed to demonstrate ocular dominance columns in *Saimiri*, Hubel and Wiesel (1978) have presented physiological evidence that there is some degree of ocular dominance segregation in *Saimiri*, but it is not as well defined as in other monkeys.

Next, an attempt was made to confirm the results of these anterograde experiments by restricting HRP to the superficial layers of the striate cortex. In using this approach, a compromise between two conflicting goals must be reached. The injection must be limited in the vertical dimension (for example, restricted to only a few layers) but must cover a large enough surface area to produce a significant number of labeled cells in the lateral genicu-

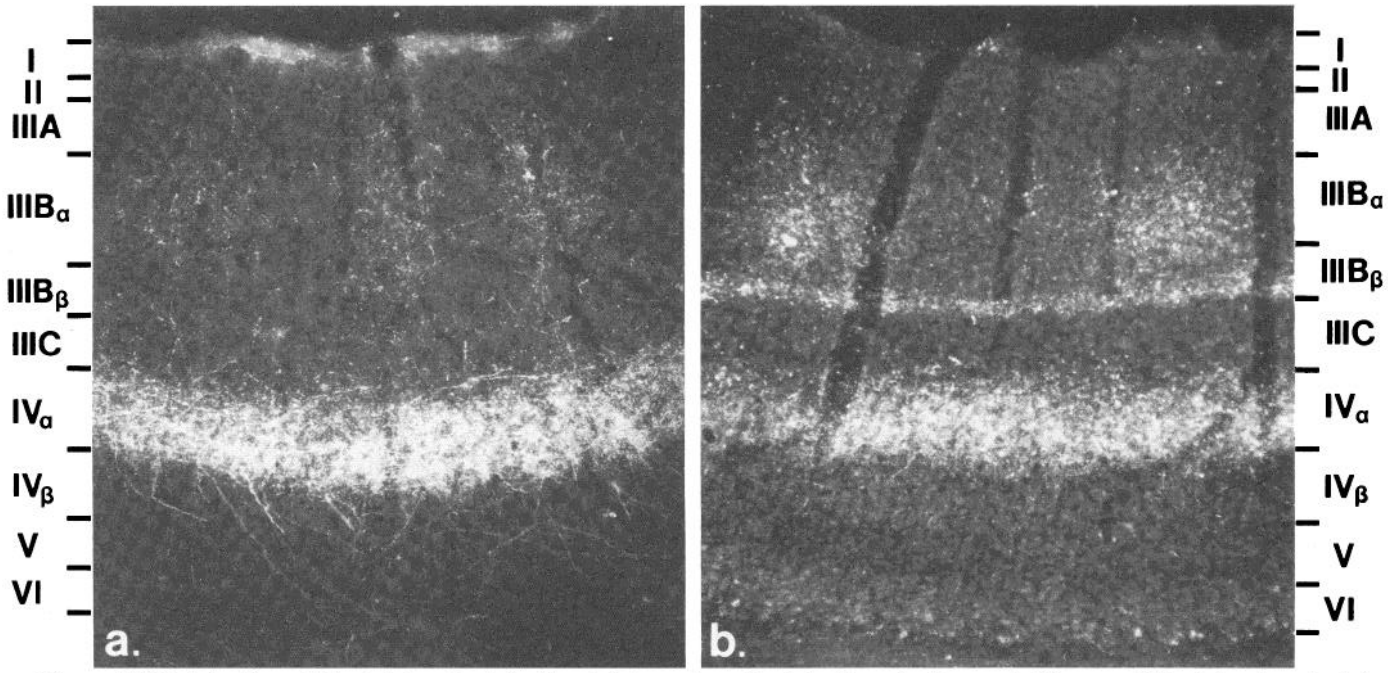

Figure 15. Distribution of labeled terminals in the striate cortex after injections in the ventral layers of the lateral geniculate body. *a*, From case 2226R. This case shows a patchy distribution of terminals in $IIIB_{\alpha}$, light terminals in layer *I*, and a dense projection to IV_{α}. Few labeled terminals were found at the base of $IIIB_{\beta}$ (× 50). *b*, From case 2288R. This case shows patches in $IIIB_{\alpha}$, a prominent band in $IIIB_{\beta}$ and IV_{α} (× 50).

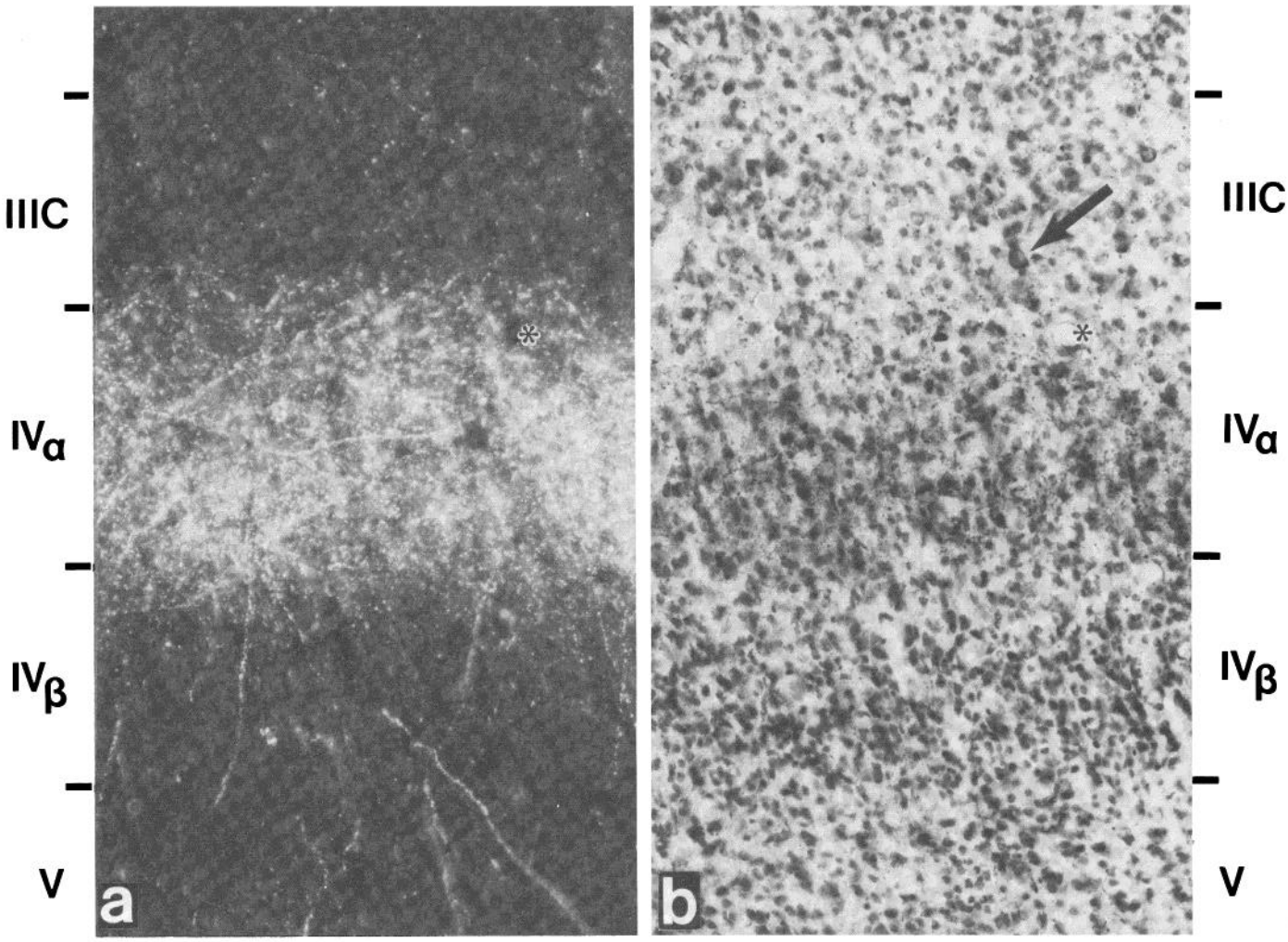

Figure 16. Distribution of terminals from the magnocellular layers of the lateral geniculate body in relation to the cytoarchitecture of the striate cortex. Darkfield (*a*) and lightfield (*b*) photomicrographs from the striate cortex of case 2226R. The *arrow* points to a large cell body which defines the lower border of *IIIC*. Terminals from the lateral geniculate body end just below the level of this cell. *Asterisks* indicate the same blood vessel in both photomicrographs (× 170).

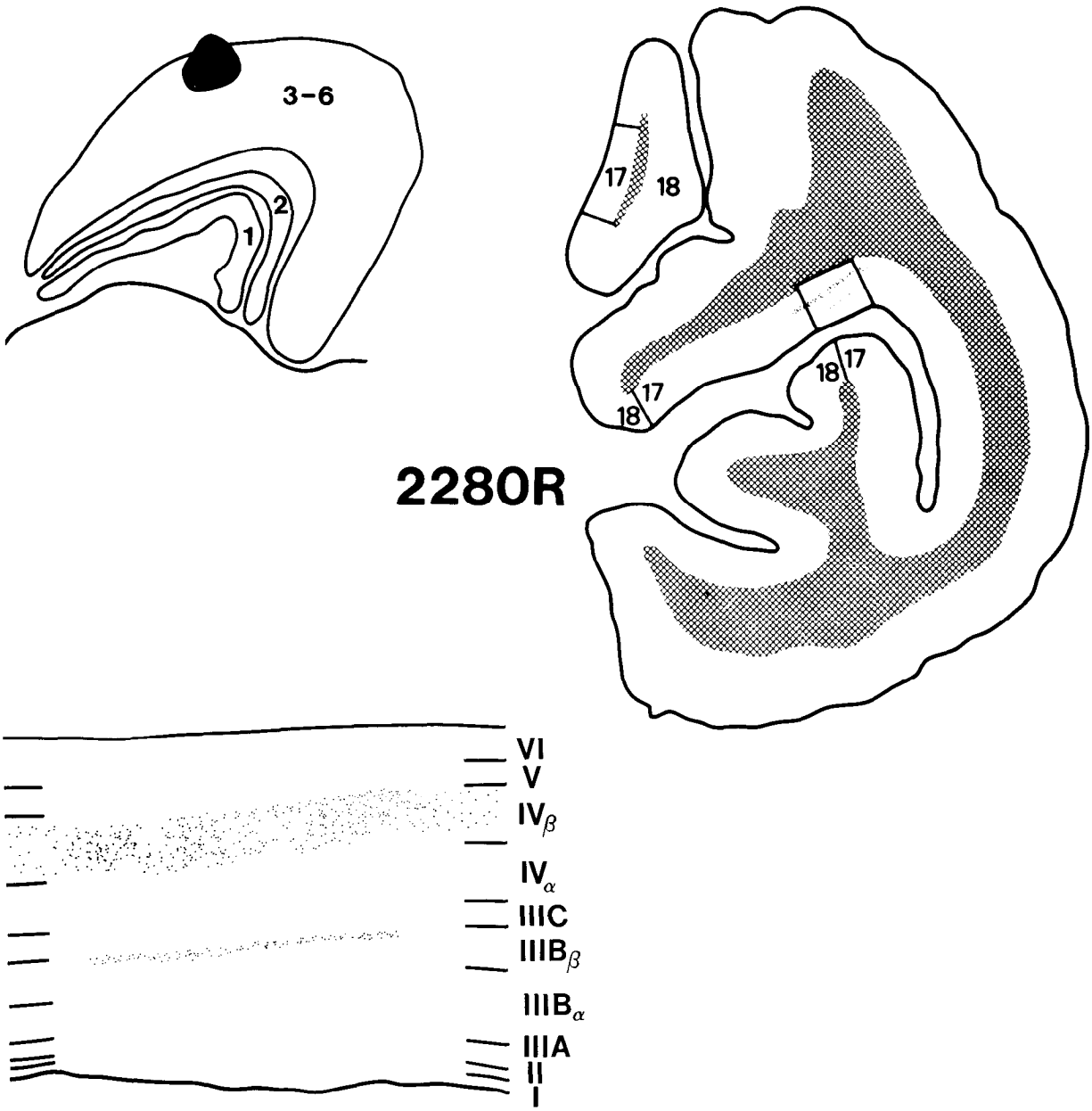

Figure 17. Case *2280R*: Results of an injection of WGA-HRP into the parvocellular layers of the lateral geniculate body. A photomicrograph of the injection site is shown in Figure 11.

late nucleus. Our compromise was to place two or more injections of HRP (see "Materials and Methods") within a space of 1 to 2 mm.

When HRP was restricted to the area dorsal to the zone of geniculate terminals in IIIB$_\beta$, labeled cells were found predominantly in the intercalated layers of the lateral geniculate body. Figure 22 shows an example of one such experiment. A photomicrograph of one of the injection sites from this case is shown in Figure 23. From the superficial injection site, labeled fibers can be seen running through IIIB and into IIIC where large numbers of labeled terminals are found. Additional fibers course through layer IV into layer V, where a second conspicuous zone of terminals is found. In addition to labeled terminals, labeled cells are also present within these regions. Layer IV is conspicuously free of labeled cells or terminals.

Following this injection, 49 cells were labeled in the lateral geniculate body. Of these cells, 43% were in the internal intercalated layer, 51% were in the external intercalated layer, and 6% were in the parvocellular layers. No labeled cells were found in the magnocellular layers. We conclude that the labeled terminals found in the superficial layers of the striate cortex can be attributed largely to cells within the intercalated layers.

Our interpretation depends upon an accurate assessment of the injection site. In order to test the interpretation of the ventral extent of the injection site and to verify the source of the terminals within the ventral portion of IIIB$_\beta$, an attempt was made to produce an

injection of HRP which included the base of IIIB$_\beta$. Figure 24 shows an example of such an experiment. In this experiment, the two injections were centered in IIIB$_\beta$ and included its base, without much involvement of IIIC. The injection site itself is instructive because it shows a different pattern of intracortical connections than that found in the more superficial injections. Labeled fibers can be seen leaving the injection site and coursing through IIIC and IV into layer V, where a cluster of labeled terminals and cell bodies are found. In contrast to the superficial injections, few labeled terminals or cell bodies were found within IIIC, whereas a good number of labeled cell bodies were found within layer IV. This suggests that cells in layer IV project predominantly to layer IIIB$_\beta$ and not to the more superficial layers.

Following these injections 16 cells were labeled in the lateral geniculate body. Of these, 11 were located within the parvocellular layers and 5 cells were located in the

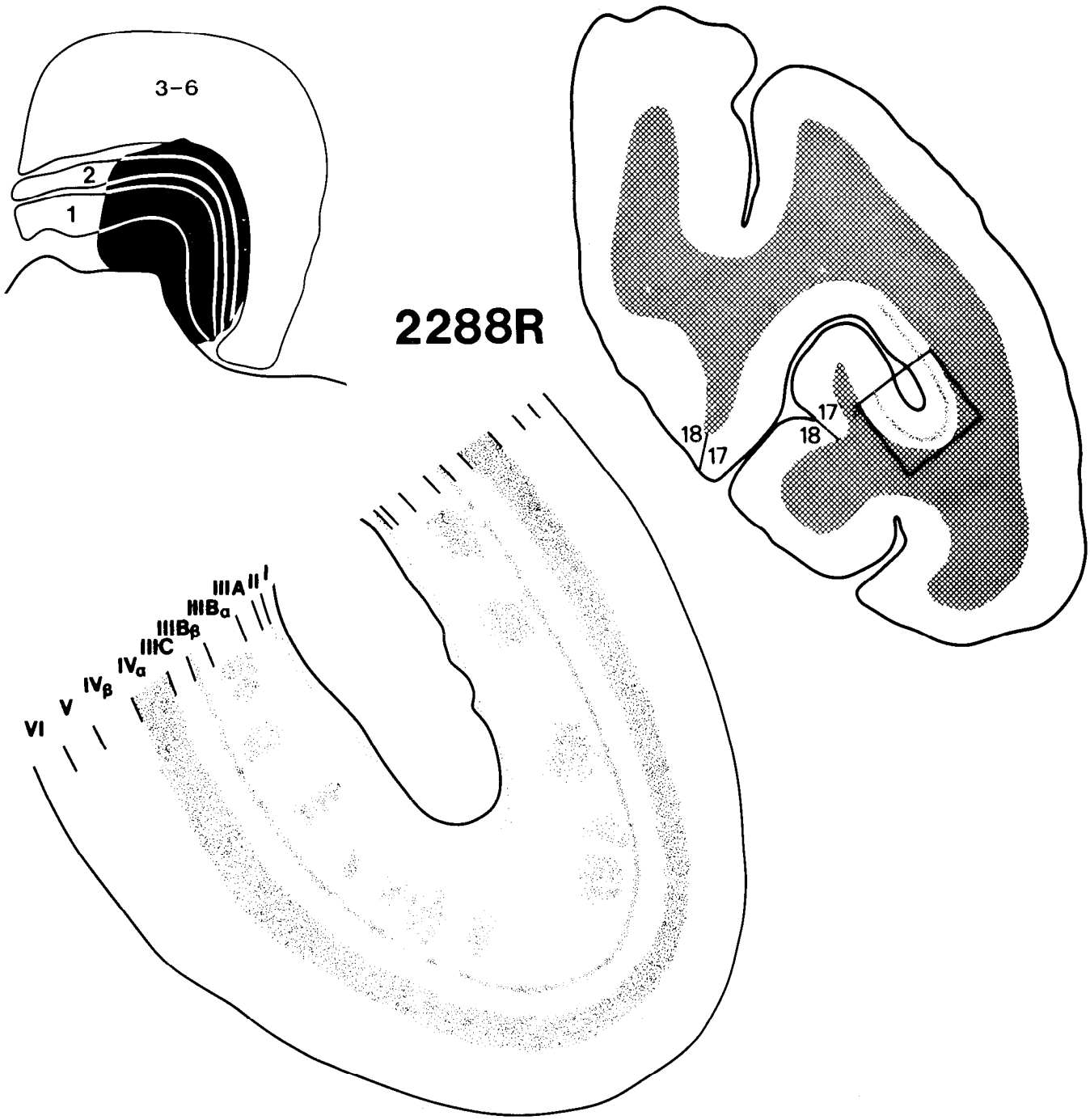

Figure 18. Case *2288R*: Results of an injection of WGA-HRP into the ventral layers of the lateral geniculate body. A photomicrograph of the injection site is shown in Figure 11, and a photomicrograph of the transport to striate cortex is shown in Figure 15*b*.

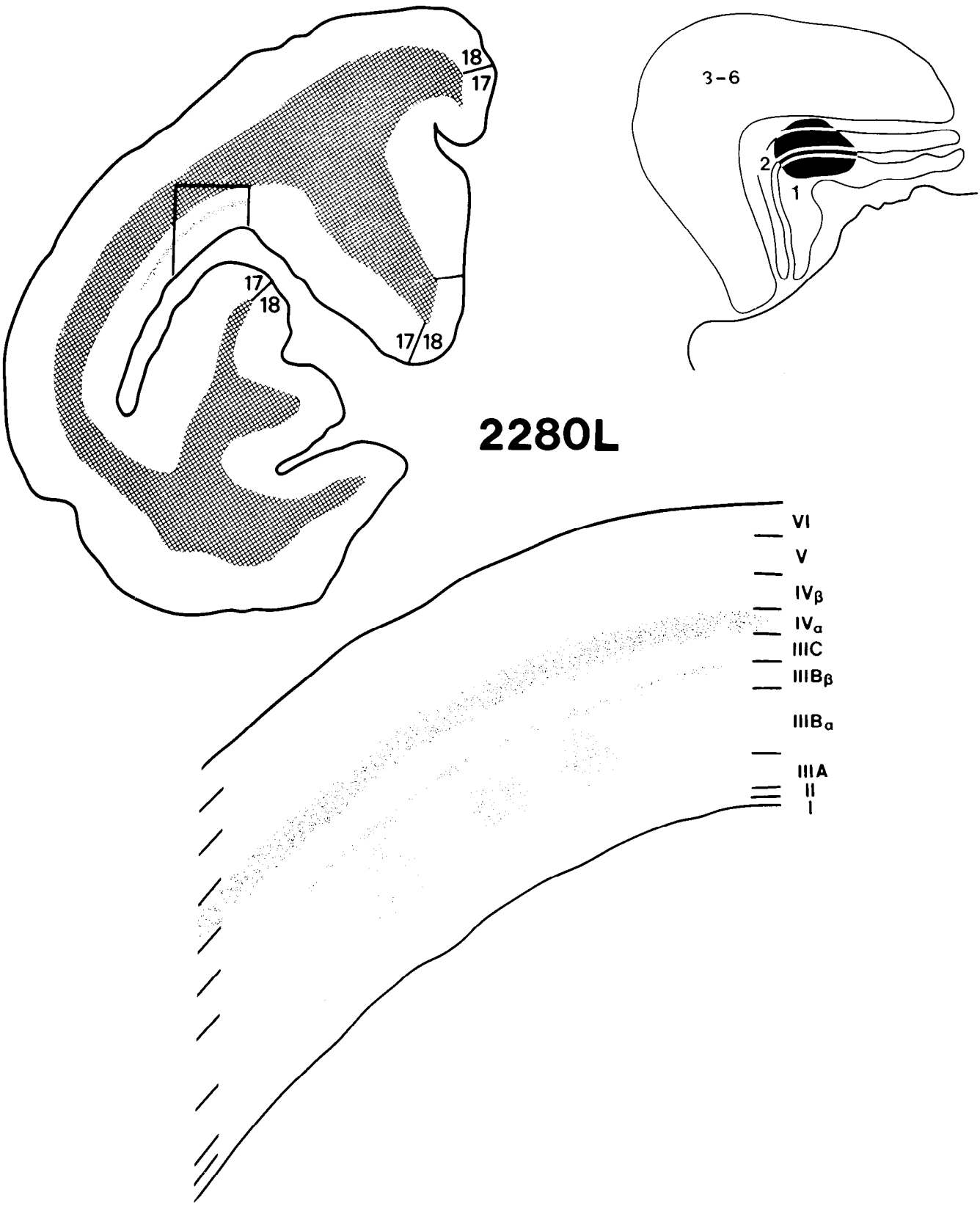

Figure 19. Case *2280L*: Results of an injection which includes the magnocellular layers and the internal intercalated layer. A photomicrograph of the injection site from this case is shown in Figure 11.

intercalated layer between layers 2 and 3. The finding that the majority of the labeled cells are in the parvocellular layers is consistent with the anterograde results showing a projection from the parvocellular layers to the base of $IIIB_\beta$ and supports our interpretation of the extent of the injection site in this and in the previous experiment. The labeled cells in the internal intercalated layer could be the result of the small encroachment of

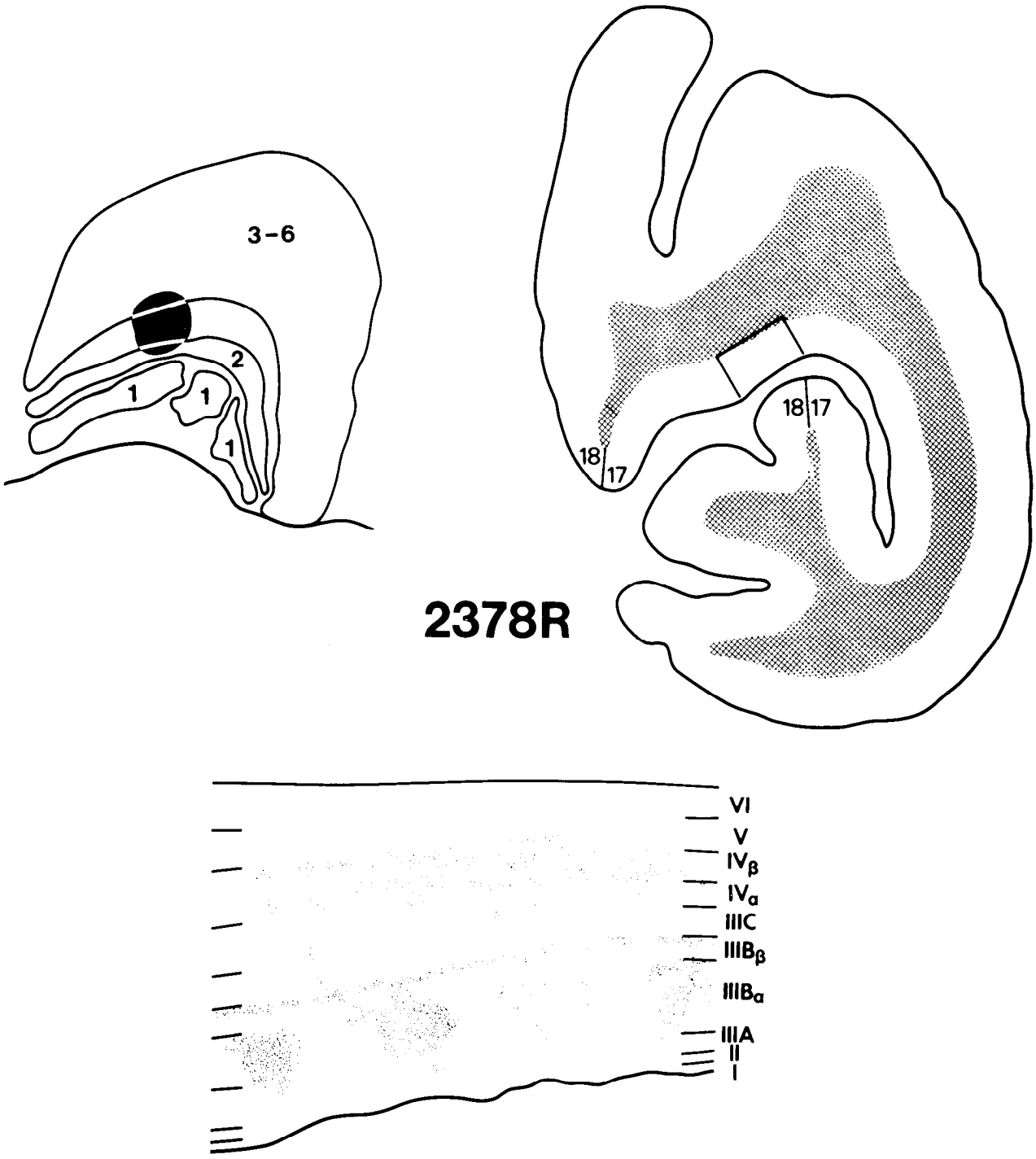

Figure 20. Case *2378R*: Results of an injection centered in the internal intercalated layer. The injection site encroaches upon parvocellular layer *3* and magnocellular layer *2*. A photomicrograph of the injection site is shown in Figure 11, and a photomicrograph of the anterograde transport to striate cortex is shown in Figure 21.

the injection site into $IIIB_{\alpha}$, the transection of axons terminating more superficially, or the fact that cells in the internal intercalated layer project to $IIIB_{\beta}$ as well as $IIIB_{\alpha}$. The last interpretation might also explain the absence of labeled cells in the external intercalated layer, since transection of axons terminating more superficially or the involvement of $IIIB_{\alpha}$ would be expected to label cells in the internal as well as the external intercalated layer.

Relation of geniculate terminal patches to metabolic markers

Recently, there have been several reports demonstrating a patchy distribution of metabolic markers (cytochrome oxidase, deoxyglucose) within the superficial layers of the striate cortex in *Saimiri* (Humphrey and Hendrickson, 1980) and *Macaca* (Horton and Hubel, 1981). Also, the distribution of glutamic acid decarbox-

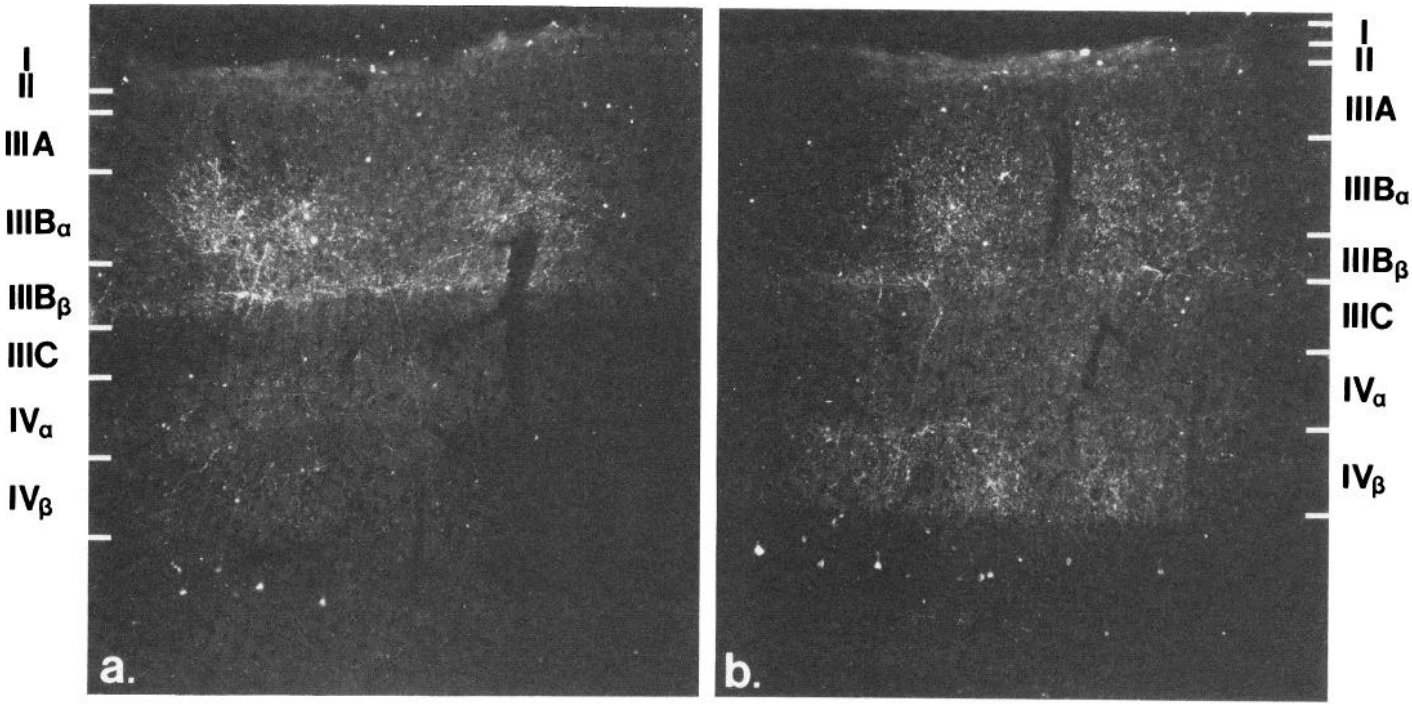

Figure 21. The distribution of terminals in the striate cortex following an injection of WGA-HRP centered in the internal intercalated layer. *a*, Distribution of terminals in the area surrounding the central zone of labeled terminals in case 2378R. There are a large number of terminals in $IIIB_\alpha$ and $IIIB_\beta$, but only a few in IV_α and IV_β (× 50). *b*, Distribution of terminals in the central zone of labeled terminals in case 2378R. Patches of labeled terminals are present in $IIIB_\alpha$ and $IIIB_\beta$. In addition sparse terminals are present in IV_α, and three well defined patches of label are present in IV_β (× 50).

ylase immunoreactivity indicative of the presence of the neurotransmitter GABA has been shown to occur in a patchy fashion (Hendrickson et al., 1981). The distance between these patches is similar to that found between geniculate terminal patches in $IIIB_\alpha$, so the obvious question is whether these two patchy patterns are coincident or interdigitating. Figure 25, *a* and *c*, shows the basic pattern of cytochrome oxidase staining in the striate cortex as reported by Humphrey and Hendrickson (1980) and Horton and Hubel (1981). The similarity with the whole pattern of geniculate inputs (Fig. 12) is compelling. The heaviest levels of cytochrome oxidase staining occur in the zones which receive geniculate input: layer IV_α and $_\beta$, the base of $IIIB_\beta$, and the patchy zone largely in $IIIB_\alpha$.

In the experiment illustrated in Figure 25, *a* and *b*, WGA-HRP was injected into the lateral geniculate body (involving all layers), and adjacent sections were processed for cytochrome oxidase staining and for peroxidase. The *asterisk* denotes a blood vessel which can be seen running through the cortex in both figures. This experiment shows that the cytochrome patches coincide precisely with the patches of terminals from the lateral geniculate body. The same conclusion, namely, that cytochrome oxidase patches are coincident with geniculate terminal patches in layer III, has been reached by M. S. Livingstone and D. H. Hubel (personal communication).

Discussion

The main significance of these results is that they provide evidence for a third visual pathway relaying in the lateral geniculate nucleus of monkeys. Earlier anatomical studies by Hubel and Wiesel (1972), Lund (1973), and Hendrickson et al. (1978) have demonstrated two pathways, one relayed by the parvocellular layers to cortical layer IV_β and the second relayed by the magnocellular layers to cortical layer IV_α; the present results confirm these findings. The present study also confirms the existence of a projection from the parvocellular layers to IVA, or in our terminology, $IIIB_\beta$. In addition to these pathways from the magnocellular and parvocellular layers, a third pathway can be defined in *Saimiri* by the following characteristics and connections: First, the size of the lateral geniculate relay cells is distinct—they are easily distinguished by size alone from those cells that are the hallmark of the magnocellular and parvocellular layers. Second, the caliber of retinal terminals in the intercalated layers is finer than the terminals in the parvocellular and magnocellular layers. Third, the intercalated layers are the main geniculate target of projections from the superficial layers of the superior colliculus (Harting et al., 1978). Finally, these layers project to the most superficial layers of striate cortex. These features taken together point to a separate and distinct pathway from retina to striate cortex.

The fine caliber of the retinal terminals in the intercalated layers has been taken as evidence that these zones receive input from a separate class of retinal ganglion cells. Support for this interpretation comes from the fact that the parvocellular C layers in the cat lateral geniculate body and layers 4 and 5 of the *Galago* lateral geniculate body are also distinguished by the fine caliber of their retinal input (Guillery, 1970; Mason and Robson, 1979; Fitzpatrick et al., 1980); and both retrograde tracing

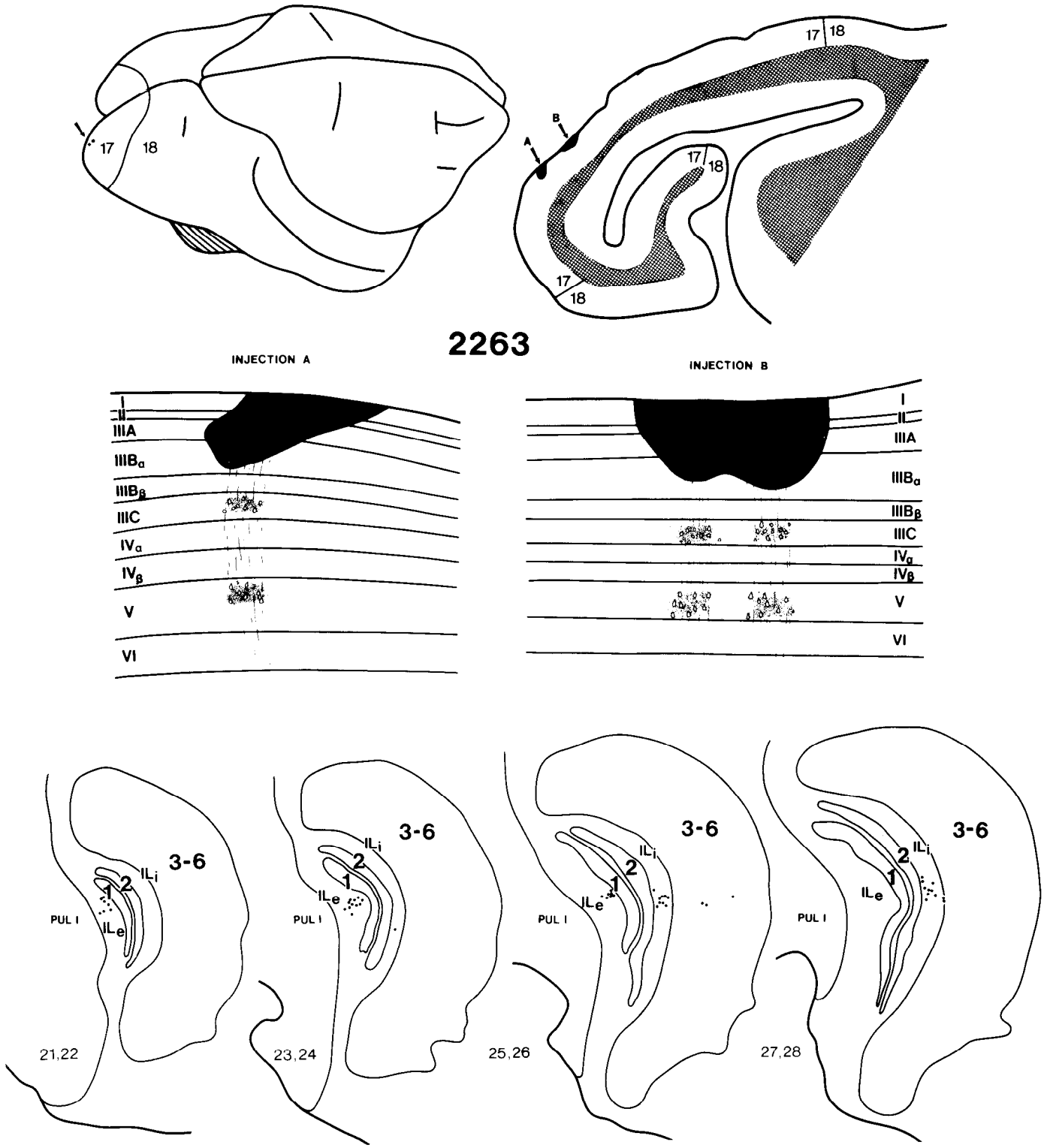

Figure 22. Case *2263*: Results of superficial injections of HRP into the striate cortex. Two separate injections were made on the dorsal surface of the striate cortex. The injection sites included *IIIB*$_\alpha$, *IIIA*, *II*, and *I*, but did not encroach upon the base of *IIIB*$_\beta$. Two prominent bands of labeled terminals were located in *IIIC* and in layer *V*. The *open triangles* in these layers indicate the presence of labeled cell bodies as well. Labeled cells in the lateral geniculate body as a result of these injections are indicated as *dots*. Each *dot* represents one labeled cell. The cells from adjacent sections were superimposed on the same drawing.

experiments and physiological studies have shown that these layers receive fibers from a distinct class of retinal ganglion cells (Wilson and Stone, 1975; Wilson et al., 1976; Itoh et al., 1981; Norton and Casagrande, 1982). There is, as yet, no physiological evidence that the intercalated layers of monkeys are the targets of a distinct type of retinal projection. But this failure may simply be related to the problems of recording from small cells, a difficulty that is compounded by the small size of the intercalated layer in comparison to the size of the mag-

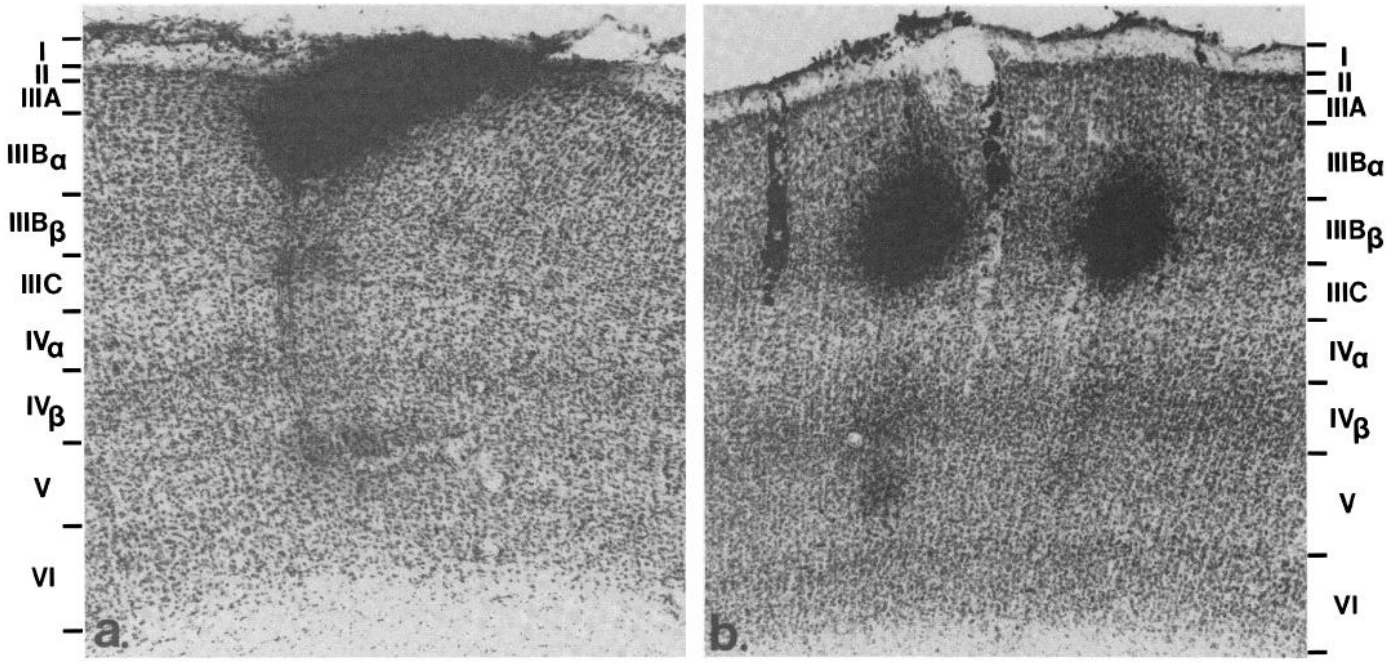

Figure 23. Injection site of HRP into the striate cortex of *Saimiri*. *a*, This is injection site A from case 2263. Labeled fibers can be seen leaving the injection site, and two bands of labeled terminals are present in *IIIC* and *V* (× 50). *b*, Injection sites in case 2320: The dark spots in layer *IV* and layer *V* are due to the presence of labeled cells and terminals (see Fig. 24) (× 50).

nocellular and parvocellular layers. The size of the intercalated layers and their relation to the principal layers would also make it very difficult to restrict a small injection of HRP only to an intercalated layer in order to determine the type of ganglion cells that project to it (see Leventhal et al., 1981). Although the evidence presented here supports the idea that the intercalated layers receive input from a distinct class of retinal ganglion cells, this hypothesis will require confirmation from an analysis of the laminar distribution of individual retino-geniculate axons.

The projection of the lateral geniculate body to the superficial layers of the striate cortex. The patchy distribution of terminals that we found in layer III was foreshadowed by earlier reports of a patchy distribution of autoradiographic grains in layer III of *Saimiri* following the injection of a transneuronal tracer into the eye (Hendrickson et al., 1978; Hubel and Wiesel, 1978) and following injections of tritiated amino acids directly into the lateral geniculate body (Weber et al., 1977). Because both WGA-HRP and ^{3}H-amino acids can be transported transneuronally, it could be argued that the labeled terminals in layer III are the result of transneuronal labeling of the axons of layer IV granule cells. Against this argument is the demonstration that HRP was transported in the retrograde direction from cortical layer IIIB$_\alpha$ to the intercalated layers of the lateral geniculate body. Furthermore, even if transneuronal transport of tracers occurred, it would not account for the patches in layer IIIB$_\alpha$ because IIIB$_\alpha$ is not a direct target of layer IV granule cells (see next section).

The present results provide support for the idea that the lateral geniculate body in monkeys projects to layer I of striate cortex. A number of earlier studies in *Macaca* using anterograde degeneration suggested that the lateral geniculate body projects to layer I (Hubel and Wiesel, 1972; Lund, 1973), but more recent anterograde transport studies did not confirm this projection (Hendrickson et al., 1978; Rezak and Benevento, 1979; see however, Weber et al., 1977). Furthermore, the interpretation of earlier degeneration experiments was complicated by the discovery that the pulvinar nucleus projects to layer I, thus raising the possibility that earlier degeneration evidence was contaminated by damage to fibers of passage (Benevento and Rezak, 1975; Ogren and Hendrickson, 1977). In the experiments presented here, a sparse distribution of labeled terminals was found in the outer portion of layer I after large injections that involved the magnocellular and surrounding intercalated layers. The labeled terminals in layer I were precisely in register with the terminals in deeper layers, and this fact alone would seem to rule out fibers of passage from the pulvinar as the source. It remains to be determined whether the same cells in the intercalated layers send axons to layer III and to layer I.

Finally, the results suggest that the internal intercalated layer as well as the parvocellular layers project to layer IIIB$_\beta$. Previous studies in *Macaca* have concluded that this projection arises exclusively from the parvocellular layers (Hubel and Wiesel, 1972; Lund, 1973; Hendrickson et al., 1978). Inasmuch as injections in the parvocellular layers label IIIB$_\beta$ without producing patches in IIIB$_\alpha$ and injections in the most ventral part of the geniculate label the patches in IIIB$_\alpha$ without the band in IIIB$_\beta$, we would predict that at least three separate geniculate axon types project to layer III: one

population which terminates only in the base of $IIIB_{\beta}$, one which terminates only in the patches, and one which distributes to both. Indeed, our observations of individual axons filled by the injection of HRP into the white matter in the squirrel monkey reveal that some axons project to the base of $IIIB_{\beta}$ and have collaterals that extend up to $IIIB_{\alpha}$ where they terminate in a region equivalent in size to the terminal patches from the geniculate. Other filled

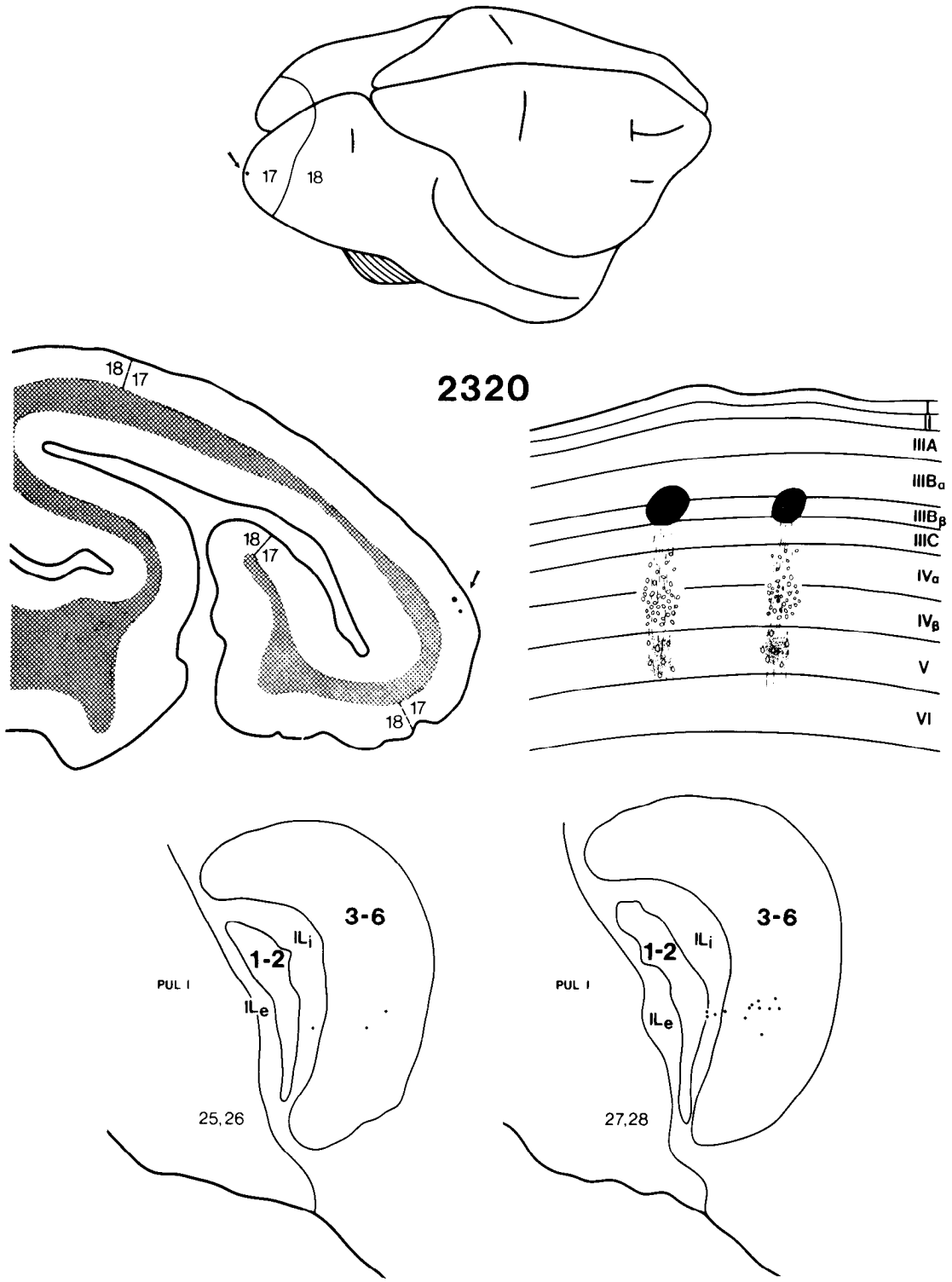

Figure 24. Case *2320*: Results of injections of HRP into layer $IIIB_{\beta}$ of the striate cortex. Two separate injections were made on the dorsal surface of the striate cortex. The injection sites were centered in $IIIB_{\beta}$ and encroached slightly into $IIIB_{\alpha}$ and *IIIC*. The *open circles* in IV_{α} and IV_{β} below the injection site indicate the presence of labeled cell bodies. Labeled cell bodies and terminals were also present in layer *V*. Labeled cells in the lateral geniculate body as a result of these injections are indicated by *dots*. Each *dot* represents one labeled cell. The cells from adjacent sections were superimposed on the same drawing.

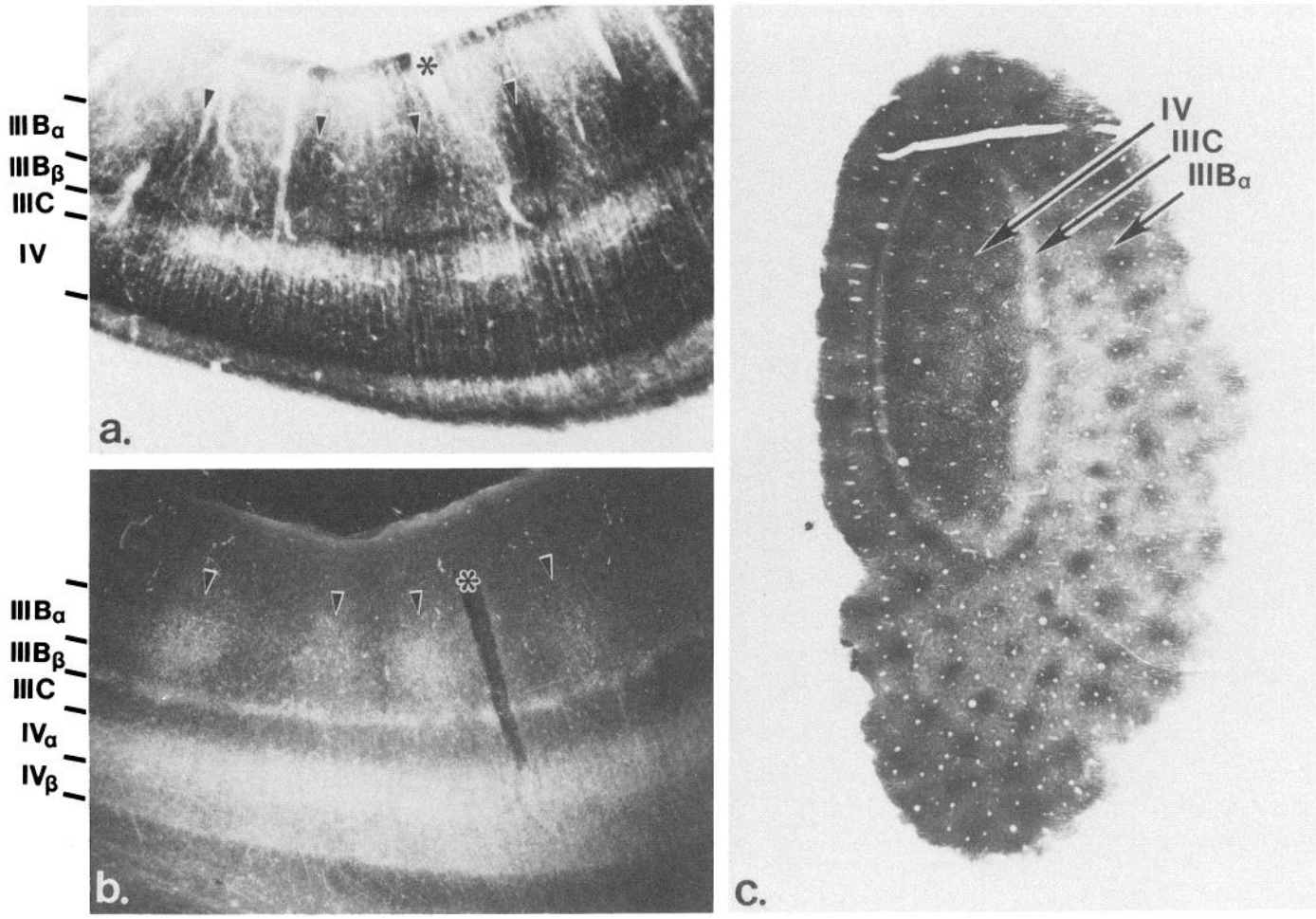

Figure 25. The distribution of cytochrome oxidase staining in the striate cortex and relation to the projections from the lateral geniculate body. *a* and *b*, Adjacent frontal sections through the striate cortex of an animal which received an injection of WGA-HRP into the lateral geniculate body. The section shown in *a* was reacted for cytochrome oxidase. The section shown in *b* was reacted for the presence of HRP. The *asterisks* denote the same blood vessel in both figures (× 30). *c*, Tangential section through the striate cortex which has been reacted for cytochrome oxidase (× 15).

axons appear to project only to $IIIB_\beta$ (D. Fitzpatrick, experiments in progress). Recently Blasdel and Lund (1982) have found individual axons in the macaque striate cortex that ascend to $IIIB_\beta$ and send a collateral to layer III as well as axons that appear restricted to the base of $IIIB_\beta$. Because none of these axons possessed a collateral to IV_β, geniculate projections to layer III and projections to layer IV may arise from entirely distinct populations of geniculate cells.

Intrinsic organization of striate cortex. Although our main goal was to examine the laminar organization of geniculate projections to striate cortex, some of these experiments shed light on the important problem of connections between different layers of striate cortex. Injections of HRP into the striate cortex which included $IIIB_\beta$ produced labeled cells within layer IV, whereas injections placed superficial to $IIIB_\beta$ did not. Thus, the main target of layer IV axons is the base of layer III whereas more superficial layers do not receive fibers directly from layer IV. This conclusion is supported by the results of Golgi studies that indicate that granule cells in layer IV of macaque send their axons to the base of IIIB (Lund, 1973; Lund and Boothe, 1975).

Injections of HRP into the most superficial layers ($IIIB_\alpha$ and above) produced labeled cells within layers IIIC and V. This result could reflect the fact that recurrent axon collaterals extend from the cells in layers V and IIIC into layer III (Lund and Boothe, 1975). But, we cannot rule out the possibility that the labeled cells were labeled by the uptake of HRP by apical dendrites.

Injections of HRP into the most superficial layers also produced labeled *terminals* in layers IIIC and V. The projection from the superficial layers to layer V has been demonstrated before in the striate cortex of primates (Spatz et al., 1970; Fisken et al., 1973; Lund and Boothe, 1975; Carey et al., 1979), and this seems to be a general feature of cortical organization inasmuch as it is also found in auditory and somatosensory cortex (Nauta et al., 1973). The presence of a dense collection of terminals in layer IIIC is a new finding not anticipated by the earlier Golgi or transport studies. It suggests that cells within the superficial layers project to IIIC as well as V.

However, since axons from area 18 terminate in both IIIC and IIIB (as well as layer I), we cannot rule out the possibility that the labeled terminals in IIIC represent HRP contained in collaterals of axons from area 18 that also project more superficially (Tigges et al., 1981; D. Fitzpatrick and K. Itoh, experiments in progress). Alternatively, these labeled terminals could be derived from axon collaterals of the cells within IIIC that also project more superficially.

Whatever the source of the terminals in IIIC, the restricted horizontal extent of the terminals in both IIIC and V, as well as the restricted labeling of cell bodies in layer IV following superficial injections, emphasizes the precise vertical organization of the connections between different layers of striate cortex. Cells within layer IV project to a restricted zone of cortex within IIIB; cells within the superficial layers send projections to layer V and possibly to layer IIIC within a restricted vertical column. These features of cortical organization are undoubtedly responsible for the similarities in receptive field position and orientation selectivity that characterize the cells found during the vertical penetration of an electrode through the striate cortex (Hubel and Wiesel, 1977).

Patchy organization of projections to layer III. The projection of the intercalated layers to patches in striate layer $IIIB_\alpha$ raises the question of the relation of this patterned input to other connections of $IIIB_\alpha$. One possibility is that this patchy pattern of afferents is related to the patchy pattern of connections between $IIIB_\alpha$ and area 18 (Tigges et al., 1977b, 1981). If, for example, the projections to area 18 originated only from the geniculate recipient zones or from the gaps between them, then we would have a good first step toward understanding the significance of the patches. But since the patchy pattern of connections with area 18 is only found after small injections of tracers into area 18 and large injections produce a continuous band of labeled cells in area 17, a correlation between the two patterns, if it exists, cannot be this simple. Since both the geniculate recipient zones and the intervening regions project to area 18, perhaps these zones project to separate populations of cells in area 18 and the patchy pattern of geniculate afferents reflects a segregation of cell types within $IIIB_\alpha$ which is maintained in the pathway from striate cortex to area 18. This idea could be tested by comparing the pattern of labeled cells and terminals in $IIIB_\alpha$ after small injections of tracers into area 18 with the pattern of cytochrome oxidase staining.

Another possibility is that the geniculate patches interdigitate with a projection which originates within the striate cortex itself. For example, the cells in IIIC may project in a discontinuous fashion upon $IIIB_\alpha$ and fill in the gaps between geniculate terminals, or the patchy pattern of local connections within $IIIB_\alpha$ may occupy the zones between geniculate patches (but see Rockland and Lund, 1982).

Finally, it is natural to think that the patchy projections from the intercalated layers to striate cortex may be related to the patchy distribution of retinal terminals in the intercalated layers. It is possible that *only* the retinal recipient zones of the intercalated layers project to the cortex and that this accounts for the patchy distribution of terminals in $IIIB_\alpha$. But there is little evidence either for or against this idea except that we never saw patches of labeled cells in the intercalated layers after HRP injections in striate cortex. In any case, inasmuch as the projections from the superior colliculus to the intercalated layers also terminate in patches, (Harting et al., 1978), it seems reasonable to suggest that tectal terminals may lie in the zones between the retinal terminal patches.

Comparison with other species. The lateral geniculate body in both prosimians and simians is characterized by readily identifiable magnocellular and parvocellular layers. The similarities in cell size, and connections of these layers in different species, along with the constant spatial relationships which these layers have to each other and to the optic tract, support the idea that they are homologous in all primates (Kaas et al., 1978). In the present report an additional class of geniculate layers has been identified in *Saimiri*, and this class is also distinguished on the basis of cell size and connections. The issues to be addressed are *whether similar intercalated layers can be identified in other primates and whether the similarities in these layers are attributable to a common ancestor.*

Layers 4 and 5 of the lateral geniculate body in the prosimian *Galago* have many features in common with the intercalated layers of *Saimiri.* These include small, pale-staining cells, projections to layers III and I of striate cortex (Carey et al., 1979; D. Fitzpatrick, M. Conley, K. Itoh, and I. T. Diamond, manuscript in preparation), projections from the superficial layers of the superior colliculus (Fitzpatrick et al., 1980), and a distinctly fine caliber retinal input which originates from small retinal ganglion cells (Fitzpatrick et al., 1980; Itoh et al., 1982). Similar small celled intercalated layers are also present in the lateral geniculate body of *Aotus.* These layers lie on either side of the magnocellular layers as well as between them. Like their counterparts in *Saimiri* and *Galago*, they receive fine caliber retinal input and project to layers III and I of striate cortex (D. Fitzpatrick, M. Conley, K. Itoh, and I. T. Diamond, manuscript in preparation).

Although there is less evidence about the presence of intercalated layers in other primate species, a review of the literature supports the idea that small celled intercalated layers are a general characteristic of the primate lateral geniculate body. The original description of small, pale-staining intercalated layers in *Macaca* has already been mentioned, and similar zones have been described in the human lateral geniculate body (Guillery and Colonnier, 1970; Hickey and Guillery, 1979). Patchy or clustered retinal projections to small-celled interlaminar zones surrounding the magnocellular layers have been shown in *Macaca* (Hubel et al., 1977; Kaas et al., 1978) and in *Callithrix* (Spatz, 1978), and there is a hint of patchy retinal terminals in these zones in the chimpanzee (Tigges et al., 1977a). The patchy distribution of retinal terminals in these species is similar to the patchy distribution of retinal projections to the intercalated layers in *Saimiri.*

The similarities in cell size, staining intensity, caliber

of retinal terminals, tectal inputs, and the laminar organization of projections to striate cortex could be taken as support for the idea that the intercalated layers in all primates are homologous. But, if these *layers* are homologous, we would expect their position to be the same in different primate species, as is the case of the magnocellular and parvocellular layers. In fact, the position of the intercalated layers varies. In most prosimians they lie between the parvocellular layers. This is true not only for the lorisiforms (for example, *Galago*), but also for the lemuriforms, such as the mouse lemur, *Microcebus* (Cooper et al., 1979). By contrast, in *Tarsier* and both new world and old world monkeys the intercalated layers occupy a more ventral position, surrounding the magnocellular layers. Even between monkey species there seems to be some variability in the position of these small cell layers. For example, in *Saimiri* they are located on either side of the magnocellular layers, whereas in *Macaca* and *Aotus* they lie between, as well as on either side of, the magnocellular layers. In addition to variability in position, there are also species differences in the organization and spatial relations of contralateral and ipsilateral retinal projections to these zones. For example, the external intercalated layer in *Saimiri* and *Callithrix* seems to receive input almost entirely from the contralateral retina, whereas this area in *Aotus* is the target of both contralateral and ipsilateral retinal projections (Kaas et al., 1978; D. Fitzpatrick, experiments in progress).

How does one reconcile the remarkable similarities in the characteristics and connections of the cells which comprise the intercalated layers with the variation in position of the layers within the geniculate? One explanation is that the similarities in the characteristics of the cells are a reflection of homology, whereas the differences, most notably the *laminar* arrangement of the cells, are independent acquisitions of the prosimian and simian lines of descent. In this view, the common ancestor of the prosimian and simian line possessed both magnocellular and parvocellular layers and, in addition, a class of cells with features characteristic of the cells in the intercalated layers. This class of cells evolved independently in different lines of descent, resulting in such differences as the location of the intercalated layers and the proportion of fibers coming from each eye. If this is true, then the well developed layers 4 and 5 of prosimians are specializations of ancestral cell type which also gave rise to the less well developed intercalated layers of primates.

An alternative explanation for the similarities in the cells which comprise the intercalated layers in primates is that they result from convergent evolution. That is to say, the common ancestor of simians and prosimians did *not* possess a cell type like that found in the intercalated layers; the cell *type*, as well as the laminar pattern, evolved independently in both lines of descent. This, of course, cannot be tested because we cannot examine the common ancestor of the simian and prosimian lines; but the idea that the common features of the cells in the intercalated layers of primates reflect common ancestry would be supported by finding similar cell types in more distantly related species (i.e., in species other than primates). The cells of layer 3 in *Tupaia* share a number of features in common with the cells of the intercalated layers of primates. These cells are distinctly small and pale staining and they receive fine caliber fibers from the retina (Glickstein, 1967; Casagrande et al., 1978). The cells in this layer are also the target of input from the tectum and the source of projections to the superficial layers of the striate cortex (Carey et al., 1979; Fitzpatrick et al., 1980). The same characteristics could be used to describe the cells in the parvocellular C layers of the cat lateral geniculate body (Guillery, 1970; Niimi et al., 1970; LeVay and Gilbert, 1975; Graham, 1977; Leventhal, 1979; Mason and Robson, 1979). It is possible that the similarities in the cells which comprise the intercalated layers as well as the segregation of this cell type into layers may have occurred independently in all of these groups; the achievements of parallel and convergent evolution are indeed remarkable, but it is unnecessary in this case to resort to parallel evolution. The more parsimonious explanation is that the cell type was present in the common ancestor of all mammals and only the segregation into layers occurred independently.

This is not to say that the cells of intercalated layers of primates, the parvocellular C layers of the cat, and layers 4 and 5 of *Galago* are identical. We already know that there are differences in the exact patterns of their afferent and efferent connections and we suspect that there may be differences in their dendritic morphology. Likewise, it is reasonable to expect species differences in the receptive field properties of these cells. We propose that differences may simply reflect the way in which a basic scheme has been modified or refined in response to distinct selective pressures in different lines of descent. Our view might be tested by examining cell types and their connections in the lateral geniculate body of generalized mammals, such as the opossum and hedgehog—species in which the lateral geniculate body has no obvious cellular lamination.

Note added in proof. Since the writing of this work, two papers relevant to this study have come to our attention (Livingstone and Hubel, 1982; Weber et al., 1983). The findings of these studies are largely in agreement with those reported here.

References

Benevento, L. A., and M. Rezak (1975) Extrageniculate projections to layers VI and I of striate cortex in rhesus monkey (*Macaca mulatta*). Brain Res. *96:* 51–55.

Blasdel, G. G., and J. S. Lund (1983) Termination of afferent axons in macaque striate cortex. J. Neurosci., in press.

Brodmann, K. (1905) Beitrage zur histologischen lokalisation der grosshirnrinde. Dritte mittelung: Die rinderfelder der niederen affen. J. Psychol. Neurol. *4:* 177–226.

Campos-Ortega, J. A.,and W. A. Hayhow (1970) A new lamination pattern in the lateral geniculate nucleus of primates. Brain Res. *20:* 335–339.

Carey, R. G., D. Fitzpatrick, and I. T. Diamond (1979) Layer I of striate cortex of *Tupaia glis* and *Galago senegalensis*: Projections from thalamus and claustrum revealed by retrograde transport of horseradish peroxidase. J. Comp. Neurol. *186:* 393–438.

Casagrande, V. A., and R. Joseph (1980) Morphological effect of monocular deprivation and recovery on the dorsal lateral

geniculate nucleus of prosimian primates. J. Comp. Neurol. *194:* 413–426.

Casagrande, V. A., R. W. Guillery, and J. K. Harting (1978) Differential effects of monocular deprivation seen in different layers of the lateral geniculate nucleus of the tree shrew (*Tupaia glis*). J. Comp. Neurol. *179:* 469–486.

Chacko, L. W. (1955) The lateral geniculate body in gibbon (*Hylobates hoolock*). J. Anat. Soc. India *4:* 69–81.

Colonnier, M., and E. Sas (1978) An anterograde degeneration study of the tangential spread of axons in cortical areas 17 and 18 of the squirrel monkey (*Saimiri sciureus*). J. Comp. Neurol. *179:* 245–262.

Cooper, H. M., H. Kennedy, M. Magnin, and F. Vital-Durand (1979) Thalamic projections to area 17 in a prosimian primate, *Microcebus murinus*. J. Comp. Neurol. *187:* 145–168.

de Olmos, J. S. (1977) An improved HRP method for the study of central nervous system connections. Exp. Brain Res. *29:* 541–551.

Ferster, D., S. LeVay (1978) The axonal arborizations of lateral geniculate neurons in the striate cortex of the cat. J. Comp. Neurol. *182:* 923–944.

Fisken, R. A., L. J. Garey, and T. P. S. Powell (1973) Patterns of degeneration after intrinsic lesions of the visual cortex (area 17) of the monkey. Brain Res. *53:* 208–213.

Fitzpatrick, D., R. G. Carey, and I. T. Diamond (1980) The projection of the superior colliculus upon the lateral geniculate body in *Tupaia glis* and *Galago senegalensis*. Brain Res. *194:* 494–499.

Giolli, R. A., and J. Tigges (1970) The primary optic pathways and nuclei in primates. In *Advances in Primatology*, C. R. Noback and W. Montagna, eds., Vol. 1, pp. 29–54, Appleton-Century-Crofts, New York.

Glendenning, K. K., E. A. Kofron, and I. T. Diamond (1976) Laminar organization of projections of the lateral geniculate nucleus to the striate cortex in *Galago*. Brain Res. *105:* 538–546.

Glickstein, M. (1967) Laminar structure of the dorsal lateral geniculate body in the tree shrew (*Tupaia glis*). J. Comp. Neurol. *131:* 93–102.

Goldman, P. S., and W. J. H. Nauta (1977) Columnar distribution of corticocortical fibers in the frontal association, limbic, and motor cortex of developing rhesus monkey. Brain Res. *122:* 393–413.

Graham, J. (1977) An autoradiographic study of the efferent connections of the superior colliculus of the cat. J. Comp. Neurol. *173:* 629–654.

Guillery, R. W. (1970) The laminar distribution of retinal fibers in the dorsal lateral geniculate nucleus of the cat: A new interpretation. J. Comp. Neurol. *138:* 339–368.

Guillery, R. W., and M. Colonnier (1970) Synaptic patterns in the dorsal lateral geniculate nucleus of the monkey. Z. Zellforsch *103:* 90–108.

Harting, J. K., I. T. Diamond, and W. C. Hall (1973) Anterograde degeneration study of the cortical projections of the lateral geniculate and pulvinar nuclei in the tree shrew (*Tupaia glis*). J. Comp. Neurol. *150:* 393–440.

Harting, J. K., V. A. Casagrande, and J. T. Weber (1978) The projection of the primate superior colliculus upon the dorsal lateral geniculate nucleus: autoradiographic demonstration of interlaminar distribution of tectogeniculate axons. Brain Res. *150:* 593–599.

Hassler, R., and A. Wagner (1965) Experimentelle und morphologische befunde ube-die vierfache corticale projektion des visuellen systems. In *Proceedings of the VIIIth International Congress of Neurology (Wien)*, Vol. III, pp. 77–96.

Hendrickson, A., J. R. Wilson, and M. P. Ogren (1978) The neuroanatomical organization of pathways between the dorsal lateral geniculate nucleus and visual cortex in old world and new world primates. J. Comp. Neurol. *182:* 123–136.

Hendrickson, A. S., S. P. Hunt, and J. -X. Wu (1981) Immunocytochemical localization of glutamic acid decarboxylase in monkey striate cortex. Nature *292:* 605–607.

Hickey, T. L., and R. W. Guillery (1979) Variability of laminar patterns in the human lateral geniculate nucleus. J. Comp. Neurol. *183:* 221–246.

Horton, J. C., and D. H. Hubel (1981) Regular patchy distribution of cytochrome oxidase staining in primary visual cortex of macaque monkey. Nature *292:* 762.

Hubel, D. H., and T. N. Wiesel (1972) Laminar and columnar distribution of geniculo-cortical fibers in the macaque monkey. J. Comp. Neurol. *146:* 421–450.

Hubel, D. H., and T. N. Wiesel (1977) Functional architecture of macaque monkey visual cortex. Proc. R. Soc. Lond. B. *198:* 1–59.

Hubel, D. H., and T. N. Wiesel (1978) Distribution of inputs from the two eyes to striate cortex of squirrel monkeys. Soc. Neurosci. Abstr. *4:* 632.

Hubel, D. H., T. N. Wiesel, and S. LeVay (1977) Plasticity of ocular dominance columns in monkey striate cortex. Phil. Trans. R. Soc. Lond. *278:* 377–409.

Humphrey, A. L., and A. E. Hendrickson (1980) Radial zones of high metabolic activity in squirrel monkey striate cortex. Soc. Neurosci. Abstr. *6:* 315.

Itoh, K., M. Conley, and I. T. Diamond (1981) Different distributions of large and small retinal ganglion cells in the cat after HRP injections of single layers of the lateral geniculate body and the superior colliculus. Brain Res. *207:* 147–152.

Itoh, K., M. Conley, and I. T. Diamond (1982) Retinal ganglion cell projections to individual layers of the lateral geniculate body in *Galago crassicaudatus*. J. Comp. Neurol. *205:* 282–290.

Kaas, J. H., M. F. Huerta, J. T. Weber, and J. K. Harting (1978) Patterns of retinal terminations and laminar organization of the lateral geniculate nucleus of primates. J. Comp. Neurol. *182:* 517–554.

Le Gros Clark, W. E. (1941) The lateral geniculate body in the platyrrhine monkeys. J. Anat. *76:* 131–140.

LeVay, S., and C. D. Gilbert (1976) Laminar patterns of geniculocortical projections in the cat. Brain Res. *113:* 1–19.

Leventhal, A. G. (1979) Evidence that different classes of relay cells of the cat's lateral geniculate nucleus terminate in different layers of the striate cortex. Exp. Brain Res. *37:* 349–372.

Leventhal, A. G., R. W. Rodieck, and B. Dreher (1981) Retinal ganglion cell classes in the old world monkey: Morphology and central projections. Science *213:* 1139–1142.

Livingstone, M. S., and D. H. Hubel (1982) Thalamic inputs to cytochrome oxidase-rich regions in monkey visual cortex. Proc. Natl. Acad. Sci. U. S. A. *79:* 6098–6101.

Lund, J. S. (1973) Organization of neurons in the visual cortex, area 17, of the monkey (*Macaca mulatta*). J. Comp. Neurol. *147:* 455–495.

Lund, J. S., and R. G. Boothe (1975) Interlaminar connections and pyramidal neuron organization in the visual cortex, area 17, of the macaque monkey. J. Comp. Neurol. *159:* 305–334.

Mason, C. A., and J. A. Robson (1979) Morphology of retinogeniculate axons in the cat. Neuroscience *4:* 79–97.

Nauta, H. J. W., A. B. Butler, and J. Jane (1973) Some observations on axonal degeneration resulting from superficial lesions of the cerebral cortex. J. Comp. Neurol. *150:* 349–360.

Niimi, K., M. Miki, and S. Kawamura (1970) Ascending projections of the superior colliculus in the cat. Okajima Folia Anat. Jpn. *47:* 269–289.

Norton, T. T., and V. A. Casagrande (1982) Laminar organization of receptive-field properties in the lateral geniculate nucleus of bushbaby (*Galago crassicaudatus*). J. Neuro-

physiol. *47:* 715–741.

Ogren, M. P., and A. E. Hendrickson (1977) The distribution of pulvinar terminals in visual areas 17 and 18 of the monkey. Brain Res. *137:* 343–350.

Rezak, M., and L. A. Benevento (1979) A comparison of the organization of the projections of the dorsal lateral geniculate nucleus, the inferior pulvinar and adjacent lateral pulvinar to primary visual cortex (area 17) in the macaque monkey. Brain Res. *167:* 19–40.

Rockland, K. S., and J. S. Lund (1982) Lattice-like intrinsic neural connections in primate striate cortex. Soc. Neurosci. Abstr. *8:* 706.

Spatz, W. B. (1977) Topographically organized reciprocal connections between areas 17 and MT (visual area of superior temporal sulcus) in the marmoset *Callithrix jacchus.* Exp. Brain Res. *27:* 559–572.

Spatz, W. B (1978) The retino-geniculo-cortical pathway in *Callithrix.* I. Intraspecific variations in the lamination pattern of the lateral geniculate nucleus. Exp. Brain. Res. *33:* 551–563.

Spatz, W. B., J. Tigges, and M. Tigges (1970) Subcortical projections, cortical associations, and some intrinsic interlaminar connections of the striate cortex in the squirrel monkey (*Saimiri*). J. Comp. Neurol. *140:* 155–174.

Tigges, J., J. Bos, and M. Tigges (1977a) An autoradiographic investigation of the subcortical visual system in the chimpanzee. J. Comp. Neurol. *172:* 367–380.

Tigges, J., M. Tigges, and A. Perachio (1977b) Complementary laminar terminations of afferents to area 17 originating in area 18 and in the lateral geniculate nucleus in squirrel monkey. J. Comp. Neurol. *176:* 87–100.

Tigges, J., M. Tigges, S. Anschel, N. A. Cross, W. D. Letbetter, and R. L. McBride (1981) Areal and laminar distribution of neurons interconnecting the central visual cortical areas 17, 18, 19 and MT in squirrel monkey (*Saimiri*). J. Comp. Neurol. *202:* 539–560.

Weber, J. T., J. H. Kaas, M. F. Huertą, and J. K. Harting (1977) Connections of the lateral geniculate nucleus (LGN) of the squirrel monkey. Soc. Neurosci. Abstr. *3:* 580.

Weber, J. T., M. F. Huerta, J. H. Kaas, and J. K. Harting (1983) The projections of the lateral geniculate nucleus of the squirrel monkey: Studies of the interlaminar zones and the S layers. J. Comp. Neurol., in press.

Wilson, P. D., and J. Stone (1975) Evidence of W-cell input to the cat's visual cortex via the C laminae of the lateral geniculate nucleus. Brain Res. *92:* 472–478.

Wilson, P. D., M. H. Rowe, and J. Stone (1976) Properties of relay cells in the cat's lateral geniculate nucleus: A comparison of W-cells with X- and Y-cells. J. Neurophysiol. *39:* 1193–1209.